eNeuro

Research Article: New Research | Neuronal Excitability

Arc controls AMPAR endocytosis through a direct interaction with clathrin-adaptor protein 2

The Arc/AP-2 interaction mediates synaptic transmission

Luis L. DaSilva[1,*], Mark J. Wall[2,*], Luciana P. de Almeida[1,4,*], Sandrine C. Wauters[2], Yunan C. Januário[1], Jürgen Müller[3,5] and Sonia A. L. Corrêa[2,4]

[1]*Ribeirão Preto Medical School, University of São Paulo, Ribeirão Preto, São Paulo, 14049-900, Brazil*
[2]*School of Life Sciences, University of Warwick, Coventry, CV4 7AL UK*
[3]*Warwick Medical School, University of Warwick, Coventry, CV4 7AL UK*
[4]*Bradford School of Pharmacy, Faculty of Life Sciences, University of Bradford, Bradford, BD7 1DP UK*
[5]*Aston Medical Research Institute, Aston Medical School, Aston University, Birmingham B4 7ET, UK*

DOI: 10.1523/ENEURO.0144-15.2016

Received: 24 November 2015

Revised: 14 April 2016

Accepted: 18 April 2016

Published: 5 May 2016

Author Contributions: L.L.d., J.M., and S.A.C. designed research; L.L.d., M.J.W., L.P.d.A., S.C.W., Y.C.J., J.M., and S.A.C. performed research; L.L.d., M.J.W., L.P.d.A., Y.C.J., and S.A.C. analyzed data; L.L.d. and S.A.C. wrote the paper.

Funding: BBSRC: BB/H018344/1. BBSRC: BB/J02127X/1. FAPESP: 2012/50147-5. FAPESP: 2009/50650-6. FAPESP: 2009/50650-6. BBSRC/GSK PhD CASE Studentship: N/A.

Conflict of Interest: Authors report no conflict of interest.

Funding sources: This work was supported by the BBSRC_FAPPA BB/J02127X/1 and BBSRC-BB/H018344/1 to SALC and by the FAPESP_RCUK_FAPPA 2012/50147-5 and FAPESP_Young Investigator's grant 2009/50650-6 to LLdS. SCW was a PhD Student supported be the BBSRC/GSK PhD-CASE Studentship, LPdA is a postdoc fellow supported by FAPESP, YCJ was supported by a FAPESP scientific initiation scholarship.

*L.L.D., M.J.W., and L.P.A. contributed equally to this work

Correspondence should be addressed to Dr. Sonia A.L. Corrêa, E-mail: s.a.l.correa@bradford.ac.uk

Cite as: eNeuro 2016; 10.1523/ENEURO.0144-15.2016

1. Manuscript Title: Arc controls AMPAR endocytosis through a direct interaction with clathrin-adaptor protein 2

2. Abbreviated Title: The Arc/AP-2 interaction mediates synaptic transmission

3. List all Author Names and Affiliations in order as they would appear in the published article: Luis L DaSilva[1#], Mark J Wall[2#], Luciana P de Almeida[1,4#],Sandrine C Wauters[2], Yunan C Januário[1], Jürgen Müller[3,5], and Sonia AL Corrêa[2,4]

[1]Ribeirão Preto Medical School, University of São Paulo, Ribeirão Preto, São Paulo, 14049-900, Brazil; [2]School of Life Sciences, University of Warwick, Coventry, CV4 7AL UK; [3]Warwick Medical School, University of Warwick, Coventry, CV4 7AL UK; [4]Bradford School of Pharmacy, Faculty of Life Sciences, University of Bradford, Bradford, BD7 1DP UK. [5]Aston Medical Research Institute, Aston Medical School, Aston University, Birmingham B4 7ET, UK

# Equal contribution

4. Author Contributions: SALC discover the Arc/AP-2 interaction, conceived the project, designed the experiments to address the importance of Arc/AP-2 regulating AMPAR trafficking, prepared hippocampal cultures and transfections for the patch-clamp experiments and wrote the manuscript. LLPdS conceived and designed the experiments to map the Arc/AP-2 interaction and its function in mammalian cells, performed experiments, analyzed and interpreted the data and helped to write the manuscript. LPdA performed and analyzed the GST pulldown and biotinylation experiments. SCW performed the immunoprecipitation experiments. MJW performed and analyzed the electrophysiological experiments. YCJ: performed experiments, analyzed and interpreted the data. JM designed the strategy to knockdown AP-2, performed the cloning of the shRNA and the production of the lentiviruses,

performed the modelling analysis of the Arc structure and contributed to the writing of the manuscript.

5. Submitting and Corresponding Author: Dr. Sonia A.L. Corrêa, E-mail: s.a.l.correa@bradford.ac.uk

6. Number of Figures: 9

7. Number of Tables: 1

8. Number of Multimedia: None

9. Number of words for Abstract: 181

10. Number of words for Significance Statement: 59

11. Number of words for Introduction: 628

12. Number of words for Discussion: 1,409

13. Acknowledgements: We wish to thank Drs Jason D Shepherd and Dawn R Collins for helpful comments on the manuscript, Dr Rodrigo O de Castro for helpful advice on the GST-pull down experiments, Dr Juan Bonifacino for providing the AP-2 core construct and Professor Jeremy M Henley for providing the myc-tagged GluA1 and GluA2 constructs.

14. Conflict of Interest: Authors report no conflict of interest

15. Funding sources: This work was supported by the BBSRC_FAPPA BB/J02127X/1 and BBSRC-BB/H018344/1 to SALC and by the FAPESP_RCUK_FAPPA 2012/50147-5 and FAPESP_Young Investigator's grant 2009/50650-6 to LLdS. SCW was a PhD Student supported be the BBSRC/GSK

PhD-CASE Studentship, LPdA is a postdoc fellow supported by FAPESP, YCJ was supported by a FAPESP scientific initiation scholarship.

Abstract

The activity-regulated cytoskeleton-associated (Arc) protein control synaptic strength by facilitating AMPA receptor (AMPAR) endocytosis. Here we demonstrate that Arc targets AMPAR to be internalized through a direct interaction with the clathrin-adaptor protein 2 (AP-2). We show that Arc overexpression overexpression in dissociated hippocampal neurons obtained from C57BL/6 mouse reduces the density of AMPAR GluA1 subunits at the cell surface and reduces the amplitude and rectification of AMPAR-mediated miniature-excitatory postsynaptic currents (mEPSC). Mutations of Arc, that prevent the AP-2 interaction reduce Arc-mediated endocytosis of GluA1 and abolish the reduction in AMPAR-mediated mEPSC amplitude and rectification. Depletion of the AP-2 subunit μ2 blocks the Arc-mediated reduction in mEPSC amplitude, effect that is restored by re-introducing μ2. The Arc/AP-2 interaction plays an important role in homeostatic synaptic scaling as the Arc-dependent decrease in mEPSC amplitude, induced by a chronic increase in neuronal activity, is inhibited by AP-2 depletion. This data provides a mechanism to explain how activity-dependent expression of Arc decisively controls the fate of AMPAR at the cell surface and modulates synaptic strength, via the direct interaction with the endocytic clathrin adaptor AP-2.

Significance Statement

The direct binding of Arc to the clathrin-adaptor protein 2 complex discovered in this study provides the crucial mechanistic link between the activity-dependent expression of Arc and the targeting of specific synaptic AMPA receptors for endocytosis. The interaction between Arc and AP-2 is crucial for many forms of synaptic plasticity and may provide a novel target for therapeutic intervention.

Introduction

Activity-dependent long-lasting alterations in glutamatergic synaptic strength are the molecular substrate thought to underlie learning and memory. The establishment and maintenance of changes in synaptic strength is dependent on trafficking of AMPAR at the postsynaptic membrane (Ehlers, 2000; Newpher and Ehlers, 2008), together with changes in protein synthesis (Buffington et al., 2014). In recent years, several neuron specific immediate early genes (IEGs) that are rapidly induced in response to neuronal activity have been described (Flavell and Greenberg, 2008), including Arc, also named activity-regulated gene of 3.1 kb (Arg3.1). Following neuronal activation, Arc mRNA is rapidly trafficked to postsynaptic dendritic sites and locally translated (Lyford et al., 1995; Steward et al., 1998). A rapid increase in Arc protein expression regulates synaptic strength, mainly by enhancing the endocytosis of AMPAR at postsynaptic sites (Rial Verde et al., 2006; Shepherd et al., 2006; Waung et al., 2008; Mabb et al., 2014). A number of studies have shown that Arc regulates several forms of synaptic plasticity, including homeostatic scaling (Shepherd et al., 2006; Corrêa et al., 2012; Mabb et al., 2014) and metabotropic glutamate receptor-dependent long-term depression (mGluR-LTD) (Waung et al., 2008; Jakkamsetti et al., 2013; Mabb et al., 2014). Arc is also required for inverse synaptic tagging. In this process, strong neuronal stimulation induces Arc expression which binds to inactive CaMKIIβ (Okuno et al., 2012). The Arc/CaMKIIβ complex then operates as a sensor to identify and induce endocytosis of AMPAR at weaker synapses thus increasing the difference between activated and non-activated synapses. Together, these findings demonstrate a pivotal role for Arc in regulating synapse strength after neuronal activation.

The clathrin-mediated endocytic (CME) pathway has been the subject of intensive studies in the past decades. Therefore, the molecular machinery involved in the sequential events linking the selection of the endocytic cargo and assembly of the clathrin scaffold leading to membrane bending and scission of the newly formed clathrin-coated vesicles has been

106 precisely described (Saheki and De Camilli, 2012; Canagarajah et al., 2013; Kirchhausen et
107 al., 2014). The clathrin-adaptor protein 2 (AP-2), which is a heterotetramer composed of two
108 large (α/β2) and two small (μ2/σ2) subunits, plays an essential role in the formation of
109 endocytic clathrin-coated vesicles (CCV). To initiate the clathrin-coat assembly the AP-2
110 complex first binds to the transmembrane cargo that is to be internalized and subsequently
111 binds and connects clathrin to the plasma membrane (Saheki and De Camilli, 2012; Traub
112 and Bonifacino, 2013; Kirchhausen et al., 2014). The sequential events observed during
113 clathrin-mediated endocytosis are conserved across different eukaryotic cell types including
114 neurons (Saheki and De Camilli, 2012). In hippocampal neurons, the cytosolic tail of the
115 AMPAR subunit 2 (GluA2) directly binds to AP-2 (Kastning et al., 2007) and disruption of the
116 AMPAR/AP-2 interaction compromises the Arc-mediated facilitation of AMPAR endocytosis
117 (Rial Verde et al., 2006).
118
119 Here we show that Arc directly binds to AP-2 and that this interaction is required for Arc-
120 mediated endocytosis of GluA1 subunits and consequent changes in synaptic transmission.
121 Under basal conditions, overexpression of Arc-wild-type (Arc-WT) reduces the amplitude
122 and rectification of AMPAR-mediated miniature excitatory postsynaptic currents (mEPSCs),
123 whereas Arc proteins bearing mutations in the AP-2 binding site, have little or no effect.
124 Furthermore, depletion of AP-2 blocks the Arc-mediated reduction in mEPSC amplitude, an
125 effect that is rescued when AP-2 expression is restored. The interaction between Arc and
126 AP-2 is also important in homeostatic synaptic scaling, as depletion of AP-2 significantly
127 reduces the Arc-dependent decrease in AMPAR mEPSC amplitude induced by increased
128 neuronal activity. The discovery that the direct interaction between Arc and AP-2 facilitates
129 rapid and sustained AMPAR endocytosis provides the mechanistic link by which constitutive
130 endocytosis can be regulated by changes in activity in neurons. These findings further
131 consolidate the strategic role of Arc in facilitating activity-dependent endocytosis of AMPAR
132 in synaptic plasticity.
133

Materials and Methods

Animals used in this study were treated in accordance with UK Animal (Scientific Procedures) Act 1986 legislation and under the appropriate national and local ethical approval. Sample size was calculated using variance from previous experiments to indicate power, with statistical significance set at 95%. Replication values are incorporated in the figures, where appropriate.

Immunoprecipitation and immunoblot analysis

To identify new proteins that interact with endogenous Arc/Arg3.1 proteins hippocampi from 10 week-old male C57BL/6 mice were used. To extract the hippocampi, animals were deeply anaesthetized and the brains were rapidly removed and placed in ice-cold artificial CSF (aCSF) consisting of (mM): 124 NaCl, 3 KCl, 26 $NaHCO_3$, 1.25 NaH_2PO_4, 2 $CaCl_2$, 1 $MgSO_4$ and 10 D-glucose (bubbled with 95% O_2 and 5% CO_2). Hippocampi were then isolated from the surrounding tissue and cut into small pieces using a dissecting microscope (Leica LED 1000). The tissue was then homogenized in Eppendorf Scientific tubes with a pellet pestle in ice-cold solution composed of: 10 mM HEPES, 0.32 M sucrose and protease inhibitor cocktail (Roche) and rotated for 1 h at 4°C. Homogenate was centrifuged at 13,000 g for 15 min, the supernatant collected and protein levels determined (BCA protein assay kit, Thermo Scientific). 500 µg of protein making 500 µl of final volume was incubated with 1 µg of rabbit polyclonal anti-Arc antibody (Synaptic Systems, 156-003) and 15 µl of pre-washed protein G agarose beads (Upstate-Millipore, 16-266) and rotated for 3 h at 4°C. As a negative control, 500 µg of protein was incubated with 15 µl with protein G agarose beads only. Arc-IP and negative control samples were centrifuged at 7000 g for 30 sec to precipitate the beads. The supernatant was removed and the beads washed 3 times with lysis buffer containing 1 mM EDTA, 1 M Tris-HCl (pH 7.5), 1% Triton X-100, 1 mM Sodium Orthovanadate, 50 mM Sodium Fluoride, Sodium pyrophosphate, 0.27 M Sucrose, 20% NaN3 and protease inhibitor cocktail (Roche). Proteins were eluted from the beads with 20 µl of 5X loading buffer, and

the total amount of the eluted protein from the beads were loaded into a 10% SDS-PAGE gels and separated for 1.5 cm using electrophoresis system.

To further confirm the endogenous interaction between Arc and AP-2 in the hippocampus, we used the co-IPs experimental conditions described above. Eluted IP proteins as well as inputs were separated in 10% SDS-PAGE gels, transferred into membrane using electrophoresis system and blots were incubated overnight with primary antibodies: rabbit anti-Arc/Arg3.1 (1:1000 dilution), mouse anti-α-adaptin1/2 (1:1000 dilution, sc-17771) and goat anti-clathrin HC (1:1000 dilution, sc-6579). Normal Rabbit IgG (1:1000; RD Systems, AB-105-C) was used as negative control for the IP experiments. Appropriate secondary antibodies were used to detect proteins levels.

Proteomics and MS analysis

Each gel lane (Arc IP and control) were cut in small pieces and subjected to in-gel tryptic digestion using a ProGest automated digestion unit (Digilab UK). The resulting peptides were fractionated using a Dionex Ultimate 3000 nanoHPLC system. Briefly, peptides in 1% (v/v) formic acid were injected onto an Acclaim PepMap C18 nano-trap column (Dionex). After washing with 0.5% (v/v) acetonitrile 0.1% (v/v) formic acid peptides were resolved on a 250 mm × 75 μm Acclaim PepMap C18 reverse phase analytical column (Dionex) over a 120 min organic gradient with a flow rate of 300 nl min−1. Peptides were ionized by nano-electrospray ionization at 2.3 kV using a stainless steel emitter with an internal diameter of 30 μm (Proxeon). Tandem mass spectrometry analysis was carried out on a LTQ-Orbitrap Velos mass spectrometer (Thermo Scientific). The Orbitrap was set to analyze the survey scans at 60,000 resolution and the top twenty ions in each duty cycle selected for MS/MS in the LTQ linear ion trap. Data was acquired using the Xcalibar v2.1 software (Thermo Scientific). The raw data files were processed and quantified using Proteome Discoverer software v1.2 (Thermo Scientific) with searches performed against the UniProt rat database by using the SEQUEST algorithm with the following criteria; peptide tolerance = 10 ppm, trypsin as the enzyme, carbamidomethylation of cysteine as a fixed modification and

oxidation of methionine as a variable modification. The reverse database search option was enabled and all data was filtered to satisfy false discovery rate (FDR) of less than 5%. Only hits from the Arc-co-IPs were considered for further characterization. The proteomics experiments were repeated twice

Hippocampal cell culture and transfection

Hippocampal neuronal cultures were prepared from either male or female postnatal day 0 pups from C57BL/6 wild-type mice as described previously (Canal et al., 2011). Briefly, hippocampi were extracted from the brain at 4°C, subject to digestion with trypsin (Sigma-Aldrich) and mechanically dissociated with DNAse (Sigma-Aldrich). Cells were plated onto 22-mm glass coverslips coated with poly-L-lysine hydrobromide (0.5mg/ml, Sigma-Aldrich). The plating medium consisted of Neurobasal-A medium (Gibco) supplemented with Gentamycin (ForMedium), L-Glutamine (ForMedium), 2% B27 (Gibco) and 5% horse serum (Gibco). The following day, the plating medium was changed for horse serum free feeding medium. Cultures were maintained at 37°C and 5% CO_2 in a humidified incubator. For immunocytochemistry and patch-clamp recordings, hippocampal cultured neurons were used at 14-16 *days in vitro* (DIV) and transfection were performed using Lipofectamine 2000 (Life technologies). For the patch-clamp recordings cells expressing Arc cDNAs were used 15-22 h after transfection and cells expressing shRNAs were transfected at 6-7 DIV and recorded at 14-16 DIV.

Cell lineages culture and transfection

Human neuroglioma 4 (H4) cells obtained from the American Type Culture Collection (Manassas, VA) were cultured in Dulbecco's modified Eagle medium (DMEM; Life technologies), supplemented with 100 U of penicillin/ml, 0.1 mg of streptomycin/ml and 10% (vol/vol) fetal bovine serum (FBS) and transiently transfected using Lipofectamine 2000 (Life technologies). Neuroblastoma x Spinal Cord (NSC) hybrid mouse cell lines (Cashman et al., 1992) cultured in supplemented DMEM were transfect with nc shRNA, µ2-shRNA$_2$, µ2-

shRNA$_3$ constructs using calcium phosphate as previously described (Canal et al., 2011). After 72-96 h of transfection, cells were washed, lysed in the presence of protease inhibitor cocktail (Roche) and 10 µg of protein were loaded onto a 10% acrylamide gel. Proteins were separated using a SDS-PAGE electrophoresis system and transferred onto Hydrobond-ECL membrane (GE healthcare). Membranes were incubated overnight with primary specific mouse anti-AP-50 µ2 subunit antibody (1:500 dilution; BD 610350), and GAPDH (1:1000 dilution; Abcam ab8245 for Figure 6) or affinity purified rabbit polyclonal anti-GAPDH antibody (1:1000 dilution; Sigma Aldrich G9545, for Figure 3). The membranes were incubated with appropriate HRP-linked secondary antibodies anti-Mouse IgG (Cell Signaling 7076), anti-Mouse IgG (NA931V GE Healthcare) or anti-rabbit IgG (NA934V GE Healthcare) incubated for 1 h at room temperature and blots developed using ECL reagents.

Recombinant DNA Constructs

Full-length mouse Arc cDNA (NM_018790.3) in pCMV-SPORT7 vector was purchased from Open Biosystems (Huntsville, AL) and used as a template to generate the Arc constructs. The pGFP-Arc plasmid was generated by cloning the Arc full length sequence as an EcoRI/SalI fragment into the pEGFP-C2 vector (Clontech). Site-directed mutagenesis (QuickChange II kit Qiagen) was used to mutate the tryptophan 197 to alanine in the pEGFP-Arc$_{(WT)}$ construct. To generate constructs encoding Arc195-199A, a synthetic cDNA sequence was obtained from GenScript (Piscataway, NJ), encoding the mouse Arc residues 1 to 700, in which codons to residues 195 to 199 (residues QSWGP) of the original Arc sequence were replaced by codons to alanine (QSWGP/AAAAA). The Arc195-199A mutant sequence was then used to replace the corresponding sequence in pGFP-ArcWT, using EcoRI and a naturally occurring BglII (nt 647-652) restriction sites. This generated the pGFP-Arc$_{(W197A)}$ and the pGFP-Arc$_{(195\text{-}199A)}$ plasmids, respectively. The plasmids encoding untagged Arc and Arc fused to mCherry (WT and mutants) were obtained by inserting the Arc cDNAs from pEGFP plasmids as EcoRI/SalI fragments into the pCIneo (Promega) or the pmCherry-C2 vectors (Clontech), respectively. To express Arc and Arc mutants in *E. coli* the full-length

Arc (WT), Arc 1-194 and Arc 1-199 sequences were amplified by PCR with specific primers and cloned into the pET28a vector using EcoRI and SalI restriction sites. The resulting plasmids encode Arc fused to a hexahistidine tag at the N-terminus. To express GST-$Arc_{(WT)}$, GST-$Arc_{(195\text{-}199A)}$ and GST-$Arc_{(W197A)}$ fusion proteins in E. coli, the Arc-WT coding sequences in pEGFP-C2 were subcloned into pGEX5.1 (GE Healthcare) as EcoRI/SalI inserts. The pcDNA3.1-μ2-mCherry vector was used to express μ2-adaptin in rescue experiments. This construct was generated using a two-step cloning strategy. Firstly, cDNA encoding mouse μ2 was amplified from pGADT7-μ2 (Guo et al., 2013) and used to replace the Leucine Zipper (LZ) sequence, in a pcDNA3.1-based plasmid consisting of a LZ sequence followed by a linker and the C-terminal (VC: 159-239) fragment of Venus YFP, provided by Dr Stephen Michnick (MacDonald et al., 2006). This construct was subsequently used to replace the VC sequence by the mCherry sequence, thus generating pcDNA3.1-μ2-mCherry. To obtain the GFP-tagged Dynamin2 (WT) construct the open reading frame of dynamin 2 was cloned into pEGFP-N1 as a HindIII and EcoRI insert. The pEGFP-C3 based plasmid encoding GFP-Triad3A was previously described (Mabb et al., 2014). All open reading frames were verified by nucleotide sequence analysis.

Recombinant protein expression and GST-pull-down assays

The four subunits of rat AP-2 complex comprising residues 1 to 621 from αC adaptin (α-trunk) fused to glutathione-S-transferase (GST) at the N-terminus, residues 1 to 591 from β2 adaptin fused to a hexahistidine tag at the C-terminus, and the full length μ2 and σ2 adaptin; (hereafter referred to as AP2 core) were co-expressed in *E. coli* BL21 Rosetta (DE3) cells from a pST39 vector (Sheffield et al., 1999) under the control of T7 promoter with each gene having its own ribosome-binding site (Chaudhuri et al., 2007; Chaudhuri et al., 2009). For GST-AP-2 core expression, bacteria were grown at 37˚C to an optical density at 600 nm of 0.8. Then cultures were shifted to 18˚C and the expression was induced with 0.2 mM IPTG (isopropyl-β-D-thiogalactopyranoside) for 12 hours. The cell pellet was re-suspended in ice-cold lysis buffer (50 mM Tris-HCl [pH 7.4], 150 mM NaCl, 10% glycerol, 2 mM EDTA, 10 mM

DTT), supplemented with 500 µg/ml lysozyme and 1 mM 4-(2-Aminoethyl) benzenesulfonyl fluoride hydrochloride (AEBSF) and disrupted by sonication. Insoluble material was removed by centrifugation and the AP-2 core in the supernatant was purified using a His-trap column (GE Healthcare). Briefly, the AP-2 core complex was bound to the His-trap column via the 6xHis-β2 subunit, repeatedly washed with Tris-buffer solution (TBS) composed of 50 mM Tris-HCl [pH 7.4], 500 mM NaCl supplemented with 30 mM of imidazol (Sigma) and eluted with TBS with 0.25 M of imidazol. Recombinant GST (pGEX plasmid), GST-$Arc_{(WT),}$ GST-$Arc_{(195\text{-}199A)}$, GST-$Arc_{(W197A)}$ and 6XHis-Arc (wild-type and truncated) were also expressed in *E. coli* BL21 Rosetta (DE3) cells at 30˚C with 0.5 mM IPTG. The pellet was re-suspended in ice-cold lysis buffer, sonicated and after centrifugation, supernatant containing the soluble proteins was used for pull-down assays.

Recombinant GST-AP-2 core or GST alone was immobilized onto glutathione-sepharose beads (GE Healthcare) overnight at 4˚C. Beads were washed with ice-cold TBS containing 5% of Triton X-100 (Sigma) and incubated with either His-trap column purified 6xHis-Arc or total cell lysates of E. coli expressing 6x-His-Arc proteins for three hours. After four washes with ice-cold TBS plus 5% of Triton X-100 the beads were re-suspended in sample buffer (SDS 4%, Tris-HCl 160 mM [pH 6.8], glycerol 20%, DTT 100 mM and bromphenol blue 0.005%), boiled and proteins were separated by SDS-PAGE and transferred onto a nitrocellulose membrane (GE Healthcare), which were then blocked for one hour with PBS, 0.1% tween 20 and 5% milk powder. Primary mouse monoclonal anti-His tag antibody (1:1000 dilution, Sigma H1029) were added in PBS, 1% BSA for one hour. After three washes with PBS-T, the membranes were incubated with HRP-conjugated secondary antibody for 1 h and washed again.

Recombinant GST, GST-$Arc_{(WT),}$ GST-$Arc_{(W197A)}$ and GST-$Arc_{(195\text{-}199A)}$ were immobilized onto glutathione-sepharose beads overnight at 4˚C. Beads were incubated with either total brain tissue lysate, obtained as described earlier for hippocampi lysate, or total lysates of HEK293 cells expressing either dynamin 2-GFP or GFP-Triad3A for 1 h at 4 °C on ice. The beads were centrifuged at 100 × g, washed three times with lysis buffer, supplemented with 1%

(v/v) Triton X-100, and subsequently resuspended in SDS-PAGE sample buffer. Beads were boiled, and proteins were resolved by SDS-PAGE and analyzed by immunoblot as described above using mouse monoclonal anti-AP-50 µ2 subunit (1:500 dilution; BD 611350)), anti-α-adaptin1/2 (1:1000 dilution, sc-17771) and rabbit polyclonal anti-GFP antibodies. Proteins were detected using ECL reagents.

Immunocytochemistry

H4 neuroglioma cells (ATCC) were transfected with plasmids encoding a myc-tag at the N-terminus of GluA1 (Leuschner and Hoch, 1999) together with plasmids encoding either mCherry, mCherry-Arc-WT or mCherry-$Arc_{(W197A)}$. 20 h after transfection, cells were fixed using 4% paraformaldehyde (PFA, pH 7.4) in 0.1 M phosphate-buffered saline (PBS) for 15 min at room temperature and incubated for 30 min at 37°C in blocking solution (0.2% pork skin gelatin) in PBS. Cells were then incubated with hybridoma culture supernatant (9E10) containing mouse monoclonal anti-myc antibody (at 1:10 dilution). Cells were washed with PBS and incubated with Alexa Fluor 488 anti-mouse IgG (1:1000; Life technologies) diluted in blocking solution. Cells were then permeabilized for 10 min with 0.1% Triton X-100 in PBS and incubated again with rabbit polyclonal anti-myc antibody (a gift from R Hegde, MRC, LMB, Cambridge, UK) for 30 min at 37°C in blocking solution. This was followed by incubation with Alexa Fluor 647 anti-rabbit IgG (1:1000; Life technologies) diluted in blocking solution. Coverslips were mounted on glass slides, and cells were imaged using a confocal laser-scanning microscope (LSM) using a Zeiss LSM 780 confocal microscope (Zeiss, Jena, Germany).

Biotinylation assays

To analyze the amount of surface and intracellular GluA1 and GluA2 proteins H4 neuroglioma cells were transfected and subject to a biotinylation protocol previously described (Eales et al., 2014). Briefly, the same amount of H4 cells were seeded in each well of six wells dishes ($3x10^5$ cells/well) and then transfected with 2 µg of plasmids encoding

N-terminus-myc-tagged GluA1 or GluA2 (Leuschner and Hoch, 1999) in combination with 2 µg of pCIneo, pCIneo-Arc$_{(WT)}$ or pCIneo-Arc$_{(W197A)}$ using lipofectamine 2000. After 24 hours the cells were washed and incubated with 1 ml of 0.25 mg/mL of EZ-Link Sulfo-NHS-SS-Biotin (Thermo Scientific) in ice-cold PBS for 15 min at 4 °C. The cells were washed twice with ice cold PBS, with 3 mL of NH4Cl 50 mM for 5 minutes (4°C on a shaker) and then once more with PBS. After washing, cells were lysed with 100 µl of lysis buffer (described above) containing protease inhibitors, rotated for 1 hour at 4°C, centrifuged at 20.000 g for 10 minutes at 4°C and the supernatants collected. The protein concentration was assayed using the BioRad Protein Assay Reagent and equal amounts were incubated with pre-washed 30 ul of NeutrAvidin® Ultra-link Resin (Life Technologies) for 3 hours on a wheel at 4°C. The beads were washed 3 times with lysis buffer, and the proteins eluted from the beads using 20 µl of 5x loading buffer. Proteins were loaded on an 8% SDS-PAGE gel. The input represents 1% of the total protein incubated with the beads. The Western blot was performed as described above.

Lentiviruses production

A lentiviral transduction system was used to achieve efficient delivery of specific microRNA-adapted shRNA sequences into neurons. Double-stranded oligonucleotides encoding shRNAs targeting the mouse µ2 subunit (shRNA1: tgctgtgaattgccctccatatggttgttttggccactgactgacaaccatatagggcaattca/ cctgtgaattgccctatatggttgtcagtcagtggccaaaacaaccatatggagggcaattcac; shRNA2: tgctgcatattggtactctattgcctgttttggccactgactgacaggcaatagtaccaatatg/ cctgcatattggtagtattgcctgtcagtcagtggccaaaacaggcaatagagtaccaatatgc; shRNA3: tgctgatctgcaggacattgcttcacgttttggccactgactgacgtgaagcagtcctgcagat/ cctgatagattcctatcaggctggtcagtcagtggccaaaaccagcctgagttaggaatctatc) were cloned into the linearized pcDNA6.2-GW/EmGFP-miR vector (Invitrogen). The sequences were designed using the "BLOCK-iT™ RNAi Designer" software from Invitrogen to identify sequences specific for mouse µ2 that are not predicted to knock down expression of any other genes. In

addition, the sequences have 100% homology to the target sequence and result in target cleavage. The vector contains flanking sequences allowing the shRNAs to be expressed and processed analogous to endogenous shRNAs. This arrangement enables the expression of the shRNA cassette from an RNA polymerase II promoter. In addition, emGFP is expressed iso-cistronically from the same promoter to allow the precise identification of the transduced cells. As a negative control, the plasmid pcDNA6.2-GW/EmGFP-miR-neg control (Invitrogen) was used. This plasmid contains an insert that forms a hairpin structure which is processed into mature shRNA, but is predicted not to target any known vertebrate gene (gaaatgtactgcgcgtggagacgttttggccactgactgacgtctccacgcagtacattt). The above expression cassettes were transferred into the lentiviral expression vector pLenti6/V5-DEST (Invitrogen) by gateway cloning. Lentiviruses were produced according to the instructions of the manufacturer (Invitrogen; Block-It HiPerform Lentiviral Pol II RNAi Expression system with emGFP; K4934). Lentivirus particles were collected from the culture supernatants, purified and concentrated by incubation with 8.5% PEG 6000 and 0.4M NaCl for 1.5 hours at 4°C, followed by centrifugation at 7000 g for 10 min (4°C). Pellets were re-dissolved in neurobasal medium.

Bicuculline incubation

To induce a chronic increase in neuronal activity, hippocampal cultures were incubated with bicuculline (40 µM, Sigma Aldrich) for 48 h prior to experimental work.

Electrophysiological recordings and analysis of AMPAR-mediated miniature excitatory postsynaptic currents (mEPSCs)

Miniature excitatory postsynaptic currents (mEPSCs) were recorded from 15-18 DIV cultured pyramidal hippocampal neurons (Mabb et al., 2014). A coverslip was transferred to the recording chamber and perfused at a constant flow rate of (2-3 min-1) with a recording solution composed of (mM): 127 NaCl, 1.9 KCl, 1 $MgCl_2$, 2 $CaCl_2$, 1.3 KH_2PO_4 , 26 $NaHCO_3$, 10 D-glucose, pH 7.4 (when bubbled with 95% O2 and 5% CO_2 , 300 mOSM) at 28-30ºC. To

isolate AMPA receptor mediated mEPSCs, tetrodotoxin (1 μM, Tocris), picrotoxin (50 μM, Sigma-Aldrich) and L-689,560 (5 μM, Tocris) were present in the recording solution. Cultured neurons were visualized using IR-DIC optics with an Olympus BX51W1 microscope and Hitachi CCD camera (Scientifica, Bedford UK). Whole-cell patch clamp recordings were made from transfected (identified by fluorescence at 488 nm) and neighboring untransfected pyramidal neurons with patch pipettes (5-8 MΩ) made from thick walled borosilicate glass (Harvard Apparatus, Edenbridge UK) filled with (mM): potassium gluconate 135, NaCl 7, HEPES 10, EGTA 0.5, phosphocreatine 10, MgATP 2, NaGTP, pH 7.2, 290 mOSM). Recordings of mEPSCs were obtained at a holding potential of -75 mV using an Axon Multiclamp 700B amplifier (Molecular Devices, USA), filtered at 3 kHz and digitized at 20 kHz (Digidata 1440A, Molecular Devices). For rectification experiments, the intracellular solution contained (mM): CsCl 135, HEPES 10, EGTA 10, Mg-ATP 2, spermine 0.1; pH 7.2 with tetraethylammonium-0H (TEA-OH); 285 mOSM. To calculate the rectification index, mEPSC recordings were made at holding potentials of -60 mV and +40 mV. Data acquisition was performed using pClamp 10 (Molecular Devices).

Analysis of mEPSCs was performed using MiniAnalysis software (SynaptoSoft, Decatur, GA). For most experiments, where the holding potential was -75 mV, events were manually analyzed and were accepted if they had an amplitude >6 pA and a faster rise than decay. For the rectification experiments, where the holding potential was -60 and +40 mV and thus mEPSCs had a smaller amplitude, events were accepted if they had an amplitude > 3 pA and a waveform with a faster rise than decay. Cumulative probability curves for mEPSC amplitude were constructed from 1000-2000 mEPSCs pooled from all recordings, with the same number of mEPSCs (150) measured from each recording (Origin, Microcal). The interval between events was measured using MiniAnalysis software. To measure mEPSC kinetics, mEPSCs within individual recordings were aligned on the half-amplitude of their rise and averaged (50-100 mEPSCs were averaged in each recording). The decay of the mean current from each recording was fitted with a single exponential (maximum likelihood, MiniAnalysis or Microcal Origin). Rise times were measured from mean currents as the time

required for the current to rise from 10 to 90 % of peak amplitude. The rectification index was calculated for each recording (peak amplitude at +40 mV divided by peak amplitude at -60 mV) and then the mean rectification index was calculated for each experimental connection. For each cell an average of 100-200 mEPSCs were analyzed. Individual mEPSCs were aligned to 50 % of the rise, averaged and then the mean amplitude was measured from the peak of this mEPSC waveform. Statistical significance was measured using the Mann-Whitney test. Where possible, comparisons were made between transfected and untransfected neighboring neurons in the same culture. For each experimental condition cells were recorded and analyzed using hippocampal cultures from 4-5 different preparations.

Statistical Analysis

Data was analyzed using Prism (Version 5.04, GraphPad) and Statistical Package for the Social Sciences 21 (IBM) software. Mann-Whitney t-tests, Kolmogorov-Smirnov test, one-way ANOVA and the corresponding post-hoc tests (Tukey or Dunn's) were performed as appropriate.

Results

Arc interacts with the AP-2 complex in neurons

Arc has been shown to regulate glutamatergic synaptic transmission by dynamically enhancing AMPAR endocytosis in postsynaptic neurons (Shepherd et al., 2006; Mabb et al., 2014). Given the importance of Arc in facilitating AMPAR endocytosis during synaptic transmission we speculated that it may play a decisive role in selecting the cargo to be internalized. To test whether Arc interacts with proteins of the clathrin-mediated endocytic (CME) machinery and whether Arc is involved in selecting the cargo to be targeted for endocytosis, we used the specific rabbit anti-Arc antibody to immunoprecipitate (IP) endogenous Arc from adult C57BL6/J mice hippocampal lysate combined with mass spectrometric analysis to identify novel Arc binding partners. The control for the IP was

obtained by incubating hippocampal lysate protein with the G-agarose beads in the absence of Arc antibody. The eluted proteins from both Arc-IP and control-IP samples were subjected to tandem mass spectrometry analysis. We only considered peptides present in the Arc-IPs for further analysis and discarded unspecific peptides present in both Arc- and control-IPs. Using this criteria we identified different subunits of the adaptor protein complex-2 (AP-2) as endogenous binding partners of Arc, including the two α adaptin isoforms: α also known as αA (19 peptides and recovery of 22.83%; NP_031484) and α2, also known as αC (11 peptides and recovery of 12.37%; NP_031485) as well as β2 (11 peptides and recovery of 12.38%; NP_082191) and μ2 (9 peptides and recovery of 20.79%; Q3TWV4). These peptides were found independently in two experimental repeats. We also found clathrin heavy chain (30 peptides and recovery of 20%; NP_001003908), dynamin 1 (10 peptides and recovery of 10.57%; NP_034195), CamKII β subunit (9 peptides and recovery of 20.48%, NP_031621) and PSD95 (2 peptides and recovery 5.77%, NP_031890). Importantly, PSD95, dynamin and CamKIIβ have previously been shown to co-IP with Arc (Lyford et al., 1995; Chowdhury et al., 2006; Okuno et al., 2012). To further confirm that Arc interacts with AP-2 endogenously, we immunoprecipitated Arc protein from hippocampal lysate as previously described and resolved the proteins using SDS-PAGE. Immunoblot analysis confirmed that Arc co-immunoprecipitates with the α subunit of the AP-2 complex (Fig. 1a,b). We observed that clathrin heavy chain also co-immunoprecipitates with Arc (Fig. 1b). This result was expected as clathrin heavy chain is known to interact with AP-2 (ter Haar et al., 2000; Edeling et al., 2006; Knuehl et al., 2006). Together these findings suggest an interaction between Arc and the proteins of the CME machinery that are responsible for selecting the cargo to be internalized. To test whether Arc directly interacts with AP-2, we performed *in vitro* GST-pull-down assays using recombinant forms of Arc-wild-type (Arc-WT) and AP-2. Previous studies used recombinant AP-2 “core” complexes to demonstrate the direct interaction between AP-2 and the cytosolic tail of transmembrane cargo proteins (Höning et al., 2005) or the HIV-1 accessory protein, Nef (Chaudhuri et al., 2007; Lindwasser

et al., 2008; Chaudhuri et al., 2009). Therefore, we produced recombinant Arc-WT fused to a hexahistidine tag and recombinant GST-tagged AP-2 core, comprising the N-terminal "trunk" domains of α and β2 subunits, plus the full-length μ2 and σ2 subunits in *E. coli*. The recombinant AP-2 core complex and Arc proteins were affinity purified (Fig. 1c) and used to show that GST-tagged AP-2 core binds mouse Arc-WT, as detected by immunoblot analysis (Fig. 1d). We then used the same GST-pull-down approach to map the region of Arc that interacts with AP-2. Our initial experiments demonstrated that a C-terminal fragment of Arc comprising residues 155 to 396 is sufficient to mediate the interaction with AP-2. We then tested whether Arc mutants bearing cumulative C-terminal deletions of 40 amino acid residues would retain the capacity to bind AP-2. Using this approach we showed that the Arc C-terminus (residues 200-396, Fig. 1e) is not essential for the Arc-AP-2 interaction, as truncated Arc missing these residues (Arc1-199) was still able to interact with AP-2 (Fig. 1f). Interestingly, deletion of a further five amino acid residues from the C-terminus of Arc (Arc1-194) was sufficient to prevent AP-2 binding (Fig. 1g). Binding of Arc recombinants to GST alone was negligible, thus confirming the specificity of the Arc/AP-2 interactions (Fig. 1d,f,g). Together these results demonstrated a direct and specific interaction of Arc with the fully assembled AP-2 core complex.

Conservative tryptophan 197 mediates the Arc/AP-2 interaction

Our GST-pull-down experiments indicate that the Arc $_{195}$QSWGP$_{199}$ amino-acid sequence is required for its interaction with AP-2. Therefore, we reasoned that a single substitution of the highly conserved tryptophan in position 197, may compromise the Arc/AP-2 interaction. To test this, we performed in vitro protein binding experiments using immobilized recombinant GST-Arc$_{(WT)}$, GST-Arc$_{(195\text{-}199A)}$ or GST-Arc$_{(W197A)}$ fusion proteins to pull-down the endogenous α or μ2 subunit of AP-2 from total brain tissue lysates. We detected a robust interaction between GST-Arc$_{(WT)}$ and μ2 (Fig. 2a). However this interaction was dramatically reduced when GST-Arc$_{(W197A)}$, Arc$_{(195\text{-}199A)}$ or GST alone were used as bait (Fig. 2a), indicating that W197 is crucially involved in the interaction with AP-2. It was previously shown that Arc

493 interacts with dynamin-2 and that an internal deletion of 195-214 aa in Arc disrupt this
494 interaction (Chowdhury et al., 2006). To test the capacity of $Arc_{(W197A)}$ to interact with
495 dynamin, we performed similar in *in vitro* binding analyses using immobilized GST-$Arc_{(WT)}$ or
496 GST-$Arc_{(W197A)}$ to pull-down GFP-dynamin-2 from HEK293 cell lysates. We confirmed that
497 $Arc_{(WT)}$ binds to dynamin, however there is a significant reduction in the interaction between
498 $Arc_{(W197A)}$ mutant and dynamin (Fig. 2b). In contrast, the Arc mutants carrying alanine
499 substitutions in the AP-2 binding motif still interact with the RING domain of the ubiquitin
500 ligase Triad3A/RNF216 (Fig. 2c), a protein recently described to interact with Arc (Mabb et
501 al., 2014). Binding of $Arc_{(W197A)}$ and $Arc_{(195\text{-}199A)}$ to Triad3A indicates that these alanine
502 mutations do not cause gross conformational changes in Arc which could prevent protein-
503 protein interaction.
504
505 *Arc-mediated internalization of GluA1 requires the Arc/AP-2 interaction*
506 $Arc_{(WT)}$ overexpression in hippocampal neurons reduces surface levels of AMPAR by
507 selectively enhancing endocytosis. We reasoned that Arc-mediated endocytosis of AMPAR
508 may be linked to its ability to interact with the endocytic adaptor AP-2. To test this, we co-
509 expressed myc-GluA1 with either $Arc_{(WT)}$ or the $Arc_{(W197A)}$ mutant in H4 human neuroglioma
510 cells, and performed biotinylation assay to monitor GluA1 and GluA2 surface expression
511 levels. As previously shown in hippocampal neurons (Chowdhury et al., 2006),
512 overexpression of Arc-WT in H4 cells resulted in a significant reduction of myc-GluA1
513 surface expression levels (Fig. 3a). Importantly, the reduction in myc-GluA1 surface
514 expression was blocked when $Arc_{(W197A)}$ mutant, that does not bind AP-2, was co-expressed
515 with myc-GluA1 (Fig. 3a). Interestingly no changes in GluA2 surface expression were
516 observed when myc-GluA2 construct was co-expressed with either $Arc_{(WT)}$ or the $Arc_{(W197A)}$
517 mutant (Fig. 3b), indicating that the GluA2 subunit is potentially less sensitive to Arc than
518 GluA1 as previously suggested by Chowdhury et al. (2006). To test whether Arc
519 overexpression induces general endocytosis of AP-2/clathrin cargo proteins, we examined
520 the surface levels of EGF receptor (EGFR) in H4 cells expressing either Arc-WT or the

$Arc_{(W197A)}$ mutant. As expected, expression of Arc has no significant effect in surface expression of EGFR (Fig. 3b). To confirm whether $Arc_{(W197A)}$ mutant had an impact on the Arc-dependent internalization of GluA1, we used the same experimental condition described above to perform immunocytochemistry to label the amount of n terminus-myc-tagged GluA1 expressed at the surface. Confocal microscopy analyses confirmed that $Arc_{(WT)}$ overexpression promotes a significant reduction of the GluA1 expression at the cell surface, an effect that is impaired in cells expressing the $Arc_{(W197A)}$, that cannot bind to AP-2 (Fig. 3c-g). Together, these results indicate that Arc/AP-2 interaction is required to facilitate AMPAR internalization.

The Arc/AP-2 interaction regulates AMPAR-mediated synaptic currents

Previous findings have demonstrated that under basal conditions hippocampal cultured neurons overexpressing Arc-WT have significantly less AMPAR on their surface than neighboring untransfected neurons (Shepherd et al., 2006). There is also a significant reduction in the amplitude of AMPAR-mediated synaptic currents in CA1 neurons overexpressing Arc-WT protein in hippocampal slices (Rial Verde et al., 2006). Conversely, cultured hippocampal neurons from Arc knockout mice exhibit an increased density of AMPAR at the cell surface and a deficit in AMPAR endocytosis (Chowdhury et al., 2006). Since Arc facilitates endocytosis of AMPAR and we have demonstrated that Arc directly binds to the AP-2 complex, we predicted that the Arc/AP-2 interaction regulates expression of synaptic AMPAR. To test our prediction, we first recorded AMPAR-mediated mEPSCs from cultured hippocampal neurons overexpressing an Arc-WT-GFP-tagged construct and from untransfected neighboring cells in the same cultures. This approach was used to negate any variations in AMPAR expression which may arise from differences in cell density. Recordings from cells expressing EGFP alone were used as a control for transfection. In agreement with previous studies, a significant decrease in mEPSC amplitude was observed in cells over-expressing $Arc_{(WT)}$ compared to untransfected neighboring cells (Fig. 4a(i)); Rial Verde et al., 2006; Shepherd et al., 2006). Examination of the amplitude probability curves

549 from Fig. 4a shows that the majority of AMPAR-mediated mEPSCs had smaller amplitudes
550 in the cell where $Arc_{(WT)}$ was overexpressed (peak shifted to the left, red trace) compared to
551 the untransfected neighboring cell (black trace). In contrast, there was no significant
552 difference in the amplitude of mEPSCs recorded in an eGFP-expressing cell and its
553 untransfected neighbor (Fig. 4b(i)).
554 To test whether the Arc-mediated reduction in the AMPAR mEPSC amplitude is dependent
555 on an interaction with AP-2, we recorded mEPSCs from hippocampal cultures
556 overexpressing either $Arc_{(195\text{-}199A)}$- or $Arc_{(W197A)}$- GFP-tagged mutant constructs. As predicted,
557 the reduction in AMPAR-dependent mEPSC amplitudes observed in cells overexpressing
558 $Arc_{(W197A)}$ or $Arc_{(195\text{-}199A)}$ was significantly less pronounced when compared to cells
559 overexpressing $Arc_{(WT)}$ (Fig. 4c,d(i)).Pooled data is displayed as cumulative probability
560 distributions (Fig. 4e) and as bar charts plotting the mean amplitude and interval (Fig. 4f-g).
561 Our biochemical data shows that Arc preferentially internalises GluA1 rather than GluA2
562 subunits (Fig. 3a-b). To test whether Arc has similar effects on the endogenous AMPA
563 receptors, which are expressed at synapses, we measured the rectification of AMPA
564 receptor mediated mEPSC amplitudes. The reduction in the surface expression of synaptic
565 AMPA receptors containing GluA1 subunits would be expected to reduce rectification at
566 positive holding potentials (Bowie and Mayer, 1995; Kamboj et al., 1995; Plant et al., 2006).
567 As predicted, the rectification index (calculated by dividing the amplitude of mEPSCs at +40
568 mV by the amplitude at -60 mV) was significantly increased in cells expressing $Arc_{(WT)}$ when
569 compared to GFP and Arc_{W197A} expressing cells (Fig. 4h-i). Neither mEPSC rise or decay
570 kinetics were significantly effected by overexpression of $Arc_{(WT)}$, Arc mutants or eGFP (Fig.
571 5a-d). The consistency in mEPSC rise and decay kinetics across recordings (Fig. 5c-d)
572 demonstrates that any changes in mEPSC amplitude are a result of receptor internalisation
573 rather than variations in recording quality. These experiments suggest that the reduction in
574 mEPSC amplitude induced by $Arc_{(WT)}$ overexpression in hippocampal neurons is dependent
575 on the binding of $Arc_{(WT)}$ to the AP-2 complex.
576

577 *The AP2 subunit μ2 is required for the $Arc_{(WT)}$-induced reduction in mEPSC amplitude*

578 Previous studies have shown that depletion of the μ2 subunit compromises the stability of
579 the remaining subunits of AP-2 and also that the complexes lacking the μ2 subunit are
580 inactive and fail to localize to the plasma membrane (Meyer et al., 2000; Peden et al., 2002;
581 Motley et al., 2003). To further investigate the importance of the Arc/AP-2 interaction, we
582 designed shRNA-like sequences to knockdown the endogenous expression of μ2 in mouse
583 tissue. We then used these shRNA constructs to transfect the mouse cell line NSC-34. A
584 shRNA sequence, not predicted to knockdown any vertebrate genes, was used as a
585 negative control. Using this approach we identified two out of three shRNA sequences (μ2-
586 $shRNA_2$ and μ2-$shRNA_3$) that efficiently reduced the protein expression of μ2 in NSC-34
587 cells (Fig. 6a). To knockdown endogenous μ2 in neurons, we generated lentiviruses
588 expressing these two shRNAs. The lentiviruses also express emGFP isocistronically, to
589 efficiently identify the transduced neurons. Lentiviral transduction of μ2-$shRNA_2$ into
590 hippocampal cultures resulted in an overall 50% reduction in μ2 expression compared to the
591 negative control shRNA (Fig. 6b). Note that even under optimal circumstances transduction
592 rates in primary neurons are between 70-80% using lentiviral systems. This indicates that a
593 significantly more pronounced reduction in μ2 expression has been achieved in those cells
594 that have been transduced and used for recordings. To examine whether AP-2 is required in
595 AMPAR-mediated synaptic transmission under basal conditions, we first transduced
596 hippocampal cultures at 6-7 DIV with a lentivirus expressing μ2-$shRNA_2$-emGFP and
597 recorded AMPAR-mediated mEPSCs 7-8 days after transfection. No significant change in
598 mEPSC amplitude was observed in cells expressing μ2-$shRNA_2$ alone compared to
599 untransfected neighboring cells (Fig. 6c(i)). These findings suggest that the constitutive
600 endocytosis of AMPAR occurring under basal conditions in cultured hippocampal neurons is
601 not strictly dependent on AP-2.
602 To test whether AP-2 is required for Arc-mediated endocytosis of AMPAR, we recorded
603 mEPSCs from hippocampal neurons expressing either μ2-$shRNA_2$-emGFP- plus mCherry-
604 Arc-WT or the negative control (n.c.) shRNA-emGFP plus mCherry-Arc-WT as well as

605 untransfected neighboring neurons. Consistent with our hypothesis, a 30% reduction in
606 mEPSC amplitudes was seen in neurons expressing $Arc_{(WT)}$ plus n.c. shRNA (Fig. 6d(i)).
607 However this reduction in mEPSC amplitude was abolished in cells co-expressing Arc-WT
608 plus μ2-$shRNA_2$ (Fig. 6e(i)). Pooled data is displayed as cumulative probability distributions
609 (Fig. 6f) and as bar charts plotting the mean amplitude and interval (Fig. 6g,h). To confirm
610 this observation, we also recorded AMPAR-mediated mEPSCs from neurons expressing
611 either μ2-$shRNA_3$ alone or together with Arc-WT. Again, no change in mEPSC amplitudes
612 was seen in cells expressing μ2-$shRNA_3$ alone (Fig. 6i,j). However, expression of μ2-
613 $shRNA_3$ blocked the Arc-WT-mediated decrease in mEPSC amplitudes (Fig. 6i-k). Neither
614 mEPSC rise or decay kinetics was significantly affected by overexpression of either μ2-
615 $shRNA_2$ or μ2-$shRNA_3$ alone, Arc-WT plus μ2-$shRNA_2$ or, μ2-$shRNA_3$ or $Arc_{(WT)}$ plus n.c.
616 shRNA (Fig. 5). These results demonstrate that knockdown of the AP-2 complex is sufficient
617 to disrupt the Arc-mediated endocytosis of AMPAR. Together, these findings suggest that
618 AP-2 is required for the Arc-mediated endocytosis of AMPAR in hippocampal neurons.
619
620 *Arc-mediated reduction in AMPAR-mediated mEPSC amplitude requires the binding of Arc*
621 *to AP-2*
622 We have shown that: 1) the reduction in AMPAR-mediated mEPSC amplitude observed in
623 neurons overexpressing $Arc_{(WT)}$ is either reduced or abolished in neurons expressing
624 mutated Arc, that cannot bind to AP-2 (Fig. 4) and 2) that the effect of Arc-WT
625 overexpression on mEPSC amplitude is reduced in neurons expressing a decreased amount
626 of AP-2μ2 protein (Fig. 6). This data suggests that Arc requires AP-2 to facilitate the
627 internalization of AMPAR. To confirm the functional relationship between Arc and AP-2, we
628 recorded mEPSCs from hippocampal neurons expressing Arc-WT and μ2-$shRNA_2$-emGFP
629 in the same lentivirus combined with re-expression of μ2 using another lentivirus expressing
630 a μ2-$shRNA_2$ resistant μ2-mCherry fusion protein. As a control, lentiviruses encoding $Arc_{(195-199A)}$/
631 μ2-$shRNA_2$-emGFP and μ2-mCherry was used to transduce hippocampal cultures. As
632 predicted, the $Arc_{(WT)}$-mediated reduction in AMPAR mEPSC amplitude caused by depletion

633 of AP-2/μ2 (see Fig. 4) was reversed by overexpressing μ2 (Fig. 7a(i)), demonstrating that
634 AP-2/μ2 is specifically required for the effect of Arc on AMPAR amplitudes. In contrast, no
635 effect on AMPAR amplitudes was seen in cells expressing a mutant form of $Arc_{(195\text{-}199A)}$ that
636 cannot bind to AP-2, irrespective of the expression status of μ2 (Fig. 7b(i), c). Pooled data is
637 displayed as cumulative probability distributions (Fig. 7c) and as bar charts plotting the mean
638 amplitude and interval (Fig. 7 d-e). Neither mEPSC rise or decay kinetics were significantly
639 affected by overexpression of Arc-WT-μ2-$shRNA_2$-emGFP plus μ2-mCherry and $Arc_{(195\text{-}199A)}$-
640 μ2-$shRNA_2$-emGFP plus μ2-mCherry (Fig. 5). These experiments clearly demonstrate that
641 the Arc/AP-2 interaction is required for the reduction in AMPAR-mediated mEPSC
642 amplitudes rather than sole disruption in AP-2.
643
644 *AP-2 is required for Arc-dependent homeostatic scaling*
645 Homeostatic scaling is the ability of neurons to sense the level of synaptic activity and
646 compensate for changes by modulating their excitability. For example, in response to a
647 prolonged increase in synaptic activity, neurons reduce synaptic strength by facilitating
648 endocytosis of synaptic AMPAR (downscaling). Arc, whose expression is robustly induced
649 by increased activity, is known to facilitate synaptic downscaling by enhancing AMPAR
650 endocytosis (Shepherd et al., 2006; Mabb et al., 2014). Since we have shown that AP-2 is
651 required for the Arc-dependent endocytosis of AMPA receptors, we hypothesized that a
652 reduction in AP-2 expression should impair Arc-dependent synaptic scaling. To test this, we
653 recorded AMPAR-mediated mEPSCs from hippocampal cultured neurons chronically treated
654 with bicuculline (40 μM, 48 hr), which blocks inhibitory neurotransmission mediated by
655 $GABA_A$ receptors and thus increases neuronal firing. In agreement with previous studies
656 (Shepherd et al., 2006; Mabb et al., 2014), we observed a significant decrease in the
657 amplitude of AMPAR-dependent mEPSCs in cells incubated with bicuculline compared to
658 control cells (Fig. 8a-c). To address whether AP-2 was required for this reduction in mEPSC
659 amplitude, we reduced μ2 expression by transducing hippocampal neurons with μ2-$shRNA_2$,
660 and as a control, n.c. shRNA, for 5 days prior to bicuculline incubation. In neurons

expressing the n.c. shRNA, bicuculline incubation still resulted in a robust reduction in mEPSC amplitude (Fig. 8b,c). However, the reduction in mEPSC amplitude was significantly smaller in neurons expressing μ2-shRNA$_2$ (Fig. 8a-c). None of the treatments significantly ($p>0.05$) changed the frequency of mEPSCs (Fig. 8d) or the rise or decay kinetics of mEPSCs (Fig. 5). Together, these findings support the hypothesis that the Arc/AP-2 interaction is required for the endocytosis of AMPAR during homeostatic scaling.

Discussion

The present study identifies a functional link between Arc and the AP-2 complex, a vital component of clathrin-mediated endocytic (CME) pathway. The AP-2 complex is required for selection and recruitment of the endocytic cargo and also for clathrin recruitment to the plasma membrane, processes that initiate the formation of the clathrin-coated pit (CCP) (Robinson, 2004; Saheki and De Camilli, 2012; Kelly et al., 2014; Kirchhausen et al., 2014). Here, we demonstrate that Arc immunoprecipitates with the AP-2 complex in hippocampal lysate and that Arc directly binds to the AP-2 complex (Fig. 1). We also show that the Arc residues $_{195}$QSWGP$_{199}$ mediate the Arc/AP-2 association and that a conserved tryptophan residue at position 197 (W_{197}) is essential for this interaction (Fig. 2). Importantly, the GST-Arc mutants that is impaired in AP-2 binding still bound to another binding partner, Triad3A, demonstrating the structural integrity of the mutated Arc proteins. Interestingly, the mutated Arc proteins pulled down higher levels of Triad3A compared with GST-Arc$_{(WT)}$ from cell extracts (Fig. 2). While the reasons for these results were not addressed here, one possible explanation is that preventing the AP-2 interaction may render Arc´s C-terminal domain more accessible to make contacts with Triad3A, leading to increased binding. Importantly, this apparently higher affinity for the ubiquitin ligase Triad3A does not cause changes in the expression/stability of the Arc mutants (Fig. 3). This further demonstrates that the observed functional changes of the Arc mutants are specifically due to the loss of its binding to AP-2. In agreement with previous studies (Shepherd et al., 2006; Waung et al., 2008), we showed that overexpression of Arc strongly reduces surface expression of GluA1, but not GluA2 in

H4 neuroglioma cells (Fig. 3). In cultured hippocampal neurons, overexpression of Arc reduces the number of synaptic AMPA receptors, as shown by a decrease in the amplitude of AMPAR-mediated mEPSCs and also regulates AMPA receptor subunit composition (Fig. 4). It has been previously shown that AMPA receptors containing GluA2 subunits show a linear current-voltage relationship in contrast to GluA2-lacking receptors that show pronounced rectification (Isaac et al., 2007). In our experiments, mEPSCs recorded from neurons overexpressing GFP alone showed pronounced rectification, suggesting that the predominant combination of AMPA receptors lacks the GluA2 subunit (also see Eales et al 2014). In contrast overexpression of Arc resulted in diminished mEPSCs rectification, suggesting a reduction in the proportion of synaptic receptors that lack the GluA2 subunit. These findings are in agreement with previous studies showing that there is an increase in surface expression of GluA1, but not GluA2 subunits in hippocampal cultures obtained from Arc knockout mice at non-stimulated conditions (Shepherd et al., 2006). Also knockdown of endogenous Arc in hippocampal cultures resulted in increased GluA1 subunits at the surface at non-stimulated conditions (Waung et al., 2008). Furthermore, application of DHPG (which induces an increase in Arc translation and protein expression) to cultured hippocampal neurons reduced rectification (Eales et al., 2014). As expected, mutation of the AP-2 binding site in Arc or depletion of AP-2μ2 compromises the capacity of Arc to reduce AMPAR-mediated mEPSC amplitudes (Figs. 4-6). Furthermore, the Arc-mediated reduction in AMPAR mEPSC amplitudes was rescued in cells where depletion of AP-2μ2 was reversed by re-introducing μ2 (Fig. 7). Importantly, this rescue was compromised in cells expressing a mutated form of Arc that cannot interact with AP-2 (Fig. 7). Furthermore, disruption of the Arc/AP-2 interaction by reducing the expression of AP-2μ2 also dampens the Arc-mediated reduction in synaptic strength observed in homeostatic synaptic downscaling (Fig. 8). Combined, these experiments demonstrate that Arc-dependent endocytosis of AMPARs requires an interaction of Arc with AP-2. It has been recently shown that dynamin activity is not required to reduce AMPA receptors surface levels induced by exposure to bicuculline and potassium chloride, suggesting that homeostatic downscaling may also be induced in a

717 clathrin-independent manner (Glebov, et al., 2014). Thus we cannot discard the possibility
718 that AMPA receptor endocytosis via an as yet non-identified clathrin/dynamin independent
719 mechanism may contribute to regulate synaptic strength seen in homeostatic synaptic
720 downscaling.
721
722 The requirement of Arc regulating synaptic plasticity in the hippocampus is well-established
723 (Rial Verde et al., 2006; Bramham et al., 2010; Jakkamsetti et al., 2013; Mabb et al., 2014).
724 However, to utilize Arc as a potential therapeutic target, it would be beneficial to obtain its
725 crystal structure. During the development of this project, no information on Arc structure was
726 available. As we have discovered that the interaction between Arc and AP-2 depends on a
727 short motif in the Arc sequence (195-199), we have undertaken homology modelling studies
728 using the iTASSER suite (http://zhanglab.ccmb.med.umich.edu/I-TASSER; Roy et al., 2010)
729 to investigate the structural properties of this region and to obtain clues as to the structural
730 nature of the interaction interface. Unfortunately we were not able to obtain a model with a
731 reasonable confidence score. The main reason for this is that there are no other protein
732 structures in the databank that are sufficiently related to Arc to allow modelling by homology
733 approaches. Our attempts are in agreement with a recent study (Myrum et al., 2015) that
734 also obtained models with low scores that were deemed to be only moderately reliable. In
735 addition, the central region of the protein was suggested to be largely unstructured and
736 flexible and the area containing the AP-2 interaction motif described in this study was not
737 included in the models. Interestingly, another recent study (Zhang et al., 2015) has
738 succeeded in obtaining a partial crystal structure of Arc, demonstrating that the C-terminal
739 part of Arc is evolutionary similar to the Ty3/Gypsy retrotransposon and that it shows
740 similarity to the HIV gag protein. However, the crystal obtained does not include the N-
741 terminal sequences up to amino acid 206 and therefore does not include the AP-2 binding
742 motif. Nevertheless, as both studies (and our own modelling approach) suggested that the
743 AP-2 binding motif is in a flexible and at least partly unstructured region of the protein, it is

highly likely that this region of Arc is able to serve as a binding platform for multiple partners, including AP-2.

Arc has been shown to mediate endocytosis of AMPAR via interaction with dynamin 2 and endophilin 3, which are accessory proteins of the CME machinery (Chowdhury et al., 2006). Endophilin and dynamin are required for membrane constriction and scission of the CCV, which are late events in the CME process. Recent evidence, using mature cultured cortical neurons from distinct knockout mice where specific endophilins have been knocked out, clearly demonstrated that the assembly and early maturation events of clathrin-coated pit formation are independent of endophilin (Milosevic et al., 2011). Dynamin is recruited at late stages of endocytosis and its enrichment coincides with neck fission and release of the vesicle (Ferguson and De Camilli, 2012; Grassart et al., 2014). These findings clearly demonstrate that endophilin and dynamin do not participate in the cargo selection process. In contrast, AP-2 plays a critical role in the initiation of clathrin-mediated endocytosis, as it coordinates the cargo recruitment and selection together with clathrin recruitment and lattice assembly (Robinson, 2004; Kirchhausen et al., 2014; Kelly et al., 2014). The AP-2 complex is thought to exist in an inactive “closed” conformation in the cytosol that prevents unproductive interaction with clathrin. Binding to plasma membrane enriched phosphatidylinositol-4,5-bisphosphate [PtdIns(4,5)P2] and to transmembrane cargo, triggers conformational changes in AP-2 that are necessary to allow efficient binding to clathrin and bud formation which is thought to be the dominant mechanism for the initiation of clathrin coat assembly (Kelly et al., 2014). The current model, in which Arc is able to induce clathrin-mediated AMPAR endocytosis via interaction with endophilin and dynamin, does not place Arc as a decisive player in specifically controlling excitatory synaptic transmission. Importantly, our finding that Arc directly binds to AP-2 provides the mechanistic link by which activity-dependent expression of Arc specifically facilitates endocytosis of AMPAR. We therefore suggest a refined model where neuronal excitability induces an increase in Arc protein expression in dendritic spines (Fig. 9). Newly expressed Arc then interacts with AP-2

and possibly increases its affinity for the cytosolic tail of AMPA receptors. Activated AP-2 initiates the formation of the clathrin-mediated pits (CMP) by coordinating the assembly of clathrin and binding to AMPAR at the postsynaptic density. We speculate that following the formation of CMP, Arc then binds and recruits endophilin and dynamin, which trigger fission of the vesicle neck. Arc may not be able to simultaneously bind to AP-2 and endophilin/dynamin. Therefore, one possible explanation is that following CMP formation, the affinity between Arc and AP-2 is reduced, releasing Arc from the CMP. The unbound Arc then binds and recruits endophilin and dynamin, which promotes neck fission and release of the CCV. Alternatively, Arc binding to dynamin/endophilin may be facilitated through AP-2 interacting partners such as amphiphysin, which is able to bind to both AP-2 and dynamin (Slepnev et al., 2000). In fact, AP-2 has been described as a major hub for recruitment of accessory proteins to the maturing CMP (Schmid et al., 2006; McMahon and Boucrot, 2011). Our discovery that Arc directly binds to AP-2, which in turn regulates AMPAR endocytosis, provides the crucial mechanistic link explaining how activity-dependent expression of Arc regulates synaptic plasticity and therefore plays a critical role in learning and memory formation.

References:

Bramham CR, Alme MN, Bittins M, Kuipers SD, Nair RR, Pai B, Panja D, Schubert M, Soule J, Tiron A, Wibrand K (2010) The Arc of synaptic memory. Exp Brain Res. 200:125-40.

Bowie D, Mayer ML (1995) Inward rectification of both AMPA and kainate subtype glutamate receptors generated by polyamine-mediated ion channel block. Neuron. 15: 453-62.

Buffington SA, Huang W, Costa-Mattioli M (2014) Translational control in synaptic plasticity and cognitive dysfunction. Annu. Rev. Neurosci. 37:17-38.

797 Canagarajah BJ, Ren X, Bonifacino JS, Hurley JH (2013) The clathrin adaptor complexes as
798 a paradigm for membrane-associated allostery. Protein sci. 22:517-529.

799 Canal F, Palygin O, Pankratov Y, Corrêa SAL, Müller J. 2011. Feedback regulation of the
800 MAP kinase scafold protein KSR1 regulates synaptic plasticity in hippocampal neurons.
801 FASEB J. 25:2362-2372.

802 Cashman NR, Durham HD, Blusztajan JK, Oda K, Tabira T, Shaw IT, Dahrouge S, Antel JP
803 (1992) Neuroblastoma X Spinal-Cord (NSC) Hybrid Cell-Lines Resemble Developing Motor
804 Neurons. Dev. Dynam. 194:209-221.

805 Chaudhuri R, Lindwasser OW, Smith WJ, Hurley JH, Bonifacino JS (2007) Downregulation
806 of CD4 by human immunodeficiency virus type 1 Nef is dependent on clathrin and involves
807 direct interaction of Nef with the AP2 clathrin adaptor. J. Virol. 81:3877-3890.

808 Chaudhuri R, Mattera R, Lindwasser OW, Robinson MS, Bonifacino JS (2009) A basic patch
809 on alpha-adaptin is required for binding of human immunodeficiency virus type 1 Nef and
810 cooperative assembly of a CD4-Nef-AP-2 complex. J. Virol. 83:2518-2530.

811 Chowdhury S, Shepherd JD, Okuno H, Lyford G, Petralia RS, Plath N, Kuhl D, Huganir RL,
812 Worley PF (2006) Arc/Arg3.1 interacts with the endocytic machinery to regulate AMPA
813 receptor trafficking. Neuron. 52:445-459.

814 Correa SA, Hunter CJ, Palygin O, Wauters SC, Martin KJ, McKenzie C, McKelvey K, Morris
815 RG, Pankratov Y, Arthur JS, Frenguelli BG (2012) MSK1 regulates homeostatic and
816 experience-dependent synaptic plasticity. J. Neurosci. 32:13039-13051.

817 Eales KL, Palygin O, O'Loughlin T, Rasooli-Nejad S, Gaestel M, Müller J, Collins DR,
818 Pankratov Y, Corrêa SAL (2014) The MK2/3 cascade regulates AMPAR trafficking and
819 cognitive flexibility. Nat. Commun. 5:4701.

820 Edeling MA, Mishra SK, Keyel PA, Steinhauser AL, Collins BM, Roth R, Heuser JE, Owen
821 DJ, Traub LM (2006) Molecular switches involving the AP-2 beta2 appendage regulate
822 endocytic cargo selection and clathrin coat assembly. Dev. Cell. 10:329–342.

823 Ehlers MD (2000) Reinsertion or degradation of AMPA receptors determined by activity-
824 dependent endocytic sorting. Neuron. 28:511-525.

825 Ferguson SM, De Camilli P (2012) Dynamin, a membrane-remodelling GTPase. Nat. Rev.
826 Mol. Cell Biol. 13:75-88.

827 Flavell SW, Greenberg ME (2008) Signaling mechanisms linking neuronal activity to gene
828 expression and plasticity of the nervous system. Annu. Rev. Neurosci. 31:563-590.

829 Glebov OO, Tigaret CM, Mellor JR, Henley JM (2014) Clathrin-independent trafficking of
830 AMPA receptors. J Neurosci. 35:4830-6.

831 Grassart A, Cheng AT, Hong SH, Zhang F, Zenzer N, Feng Y, Briner DM, Davis GD, Malkov
832 D, Drubin DG (2014) Actin and dynamin2 dynamics and interplay during clathrin-mediated
833 endocytosis. J. Cell Biol. 205:721-735.

834 Guo X, Mattera R, Ren X, Chen Y, Retamal C, González A, Bonifacino JS (2013) The
835 adaptor protein-1 μ1B subunit expands the repertoire of basolateral sorting signal
836 recognition in epithelial cells. Dev. Cell. 27:353-366.

837 Höning S, Ricotta D, Krauss M, Späte K, Spolaore B, Motley A, Robinson M, Robinson C,
838 Haucke V, Owen DJ (2005) Phosphatidylinositol-(4,5)-bisphosphate regulates sorting signal
839 recognition by the clathrin-associated adaptor complex AP2. Mol. Cell. 18:519-531.

840 Isaac J T, Ashby M C, Mcbain C J (2007) The role of the GluR2 subunit in AMPA receptor
841 function and synaptic plasticity. Neuron. 54:859–71.

842 Jakkamsetti V, Tsai NP, Gross C, Molinaro G, Collins KA, Nicoletti F, Wang KH, Osten P,
843 Bassell GJ, Gibson JR, Huber KM (2013) Experience-induced Arc/Arg3.1 primes CA1

844 pyramidal neurons for metabotropic glutamate receptor-dependent long-term synaptic
845 depression. Neuron. 80:72-79.

846 Kamboj SK, Swanson GT, Cull-Candy SG (1995) Intracellular spermine confers rectification
847 on rat calcium-permeable AMPA and kainate receptors. J. Physiol. 486:297-303.

848 Kastning K, Kukhtina V, Kittler JT, Chen G, Pechstein A, Enders S, Lee SH, Sheng M, Yan
849 Z, Haucke V (2007) Molecular determinants for the interaction between AMPA receptors and
850 the clathrin adaptor complex AP-2. Proc. Natl. Acad. Sci. U.S.A. 104: 2991-2996.

851 Kelly BT, Graham SC, Liska N, Dannhauser PN, Höning S, Ungewickell EJ, Owen DJ (2014)
852 Clathrin adaptors. AP2 controls clathrin polymerization with a membrane-activated switch.
853 Science. 345:459-463.

854 Kirchhausen T, Owen D, Harrison SC (2014) Molecular structure, function, and dynamics of
855 clathrin-mediated membrane traffic. Cold Spring Harb. Perspect. Biol. 6: a016725.

856 Knuehl C, Chen CY, Manalo V, Hwang PK, Ota N, Brodsky FM (2006) Novel binding sites
857 on clathrin and adaptors regulate distinct aspects of coat assembly. Traffic. 7:1688-1700.

858 Leuschner WD, Hoch W (1999) Subtype-specific assembly of amino-3-hydroxy-5-methyl-4-
859 isoxazole propionic acid receptor subunits is mediated by their N-terminal Domains. J Biol
860 Chem. 274:16907-16.

861 Lindwasser OW, Smith WJ, Chaudhuri R, Yang P, Hurley JH, Bonifacino JS (2008) A
862 diacidic motif in human immunodeficiency virus type 1 Nef is a novel determinant of binding
863 to AP-2. J. Virol. 82:1166-1174.

864 Lyford GL, Yamagata K, Kaufmann WE, Barnes CA, Sanders LK, Copeland NG, Gilbert DJ,
865 Jenkins NA, Lanahan AA, Worley PF (1995) Arc, a growth factor and activity-regulated gene,
866 encodes a novel cytoskeleton-associated protein that is enriched in neuronal dendrites.
867 Neuron. 14:433-445.

868 Mabb AM, Je HS, Wall MJ, Robinson CG, Larsen RS, Qiang Y, Correa SA, Ehlers MD
869 (2014) Triad3A regulates synaptic strength by ubiquitination of Arc. Neuron. 82: 1299-1316.

870 MacDonald ML, Lamerdin J, Owens S, Keon BH, Bilter GK, Shang Z, Huang Z, Yu H, Dias
871 J, Minami T, Michnick SW, Westwick JK (2006) Identifying off-target effects and hidden
872 phenotypes of drugs in human cells. Nat. Chem. Biol. 2:329-337.

873 McMahon HT, Boucrot E (2011) Molecular mechanism and physiological functions of
874 clathrin-mediated endocytosis. Nat. Rev. Mol. Cell Biol.12:517-533.

875 Meyer C, Zizioli D, Lausmann S, Eskelinen EL., Hamann J, Saftig P, von Figura K, Schu P
876 (2000) mu1A-adaptin-deficient mice: lethality, loss of AP-1 binding and rerouting of mannose
877 6-phosphate receptors. EMBO J . 19:2193-2203.

878 Milosevic I, Giovedi S, Lou X, Raimondi A, Collesi C, Shen H, Paradise S, O'Toole E,
879 Ferguson S, Cremona O, De Camilli P (2011) Recruitment of endophilin to clathrin-coated pit
880 necks is required for efficient vesicle uncoating after fission. Neuron. 72:587-601.

881 Motley A, Bright NA, Seaman MN, Robinson MS (2003) Clathrin-mediated endocytosis in
882 AP-2-depleted cells. J Cell Biol. 162:909-918.

883 Myrum C, Baumann A, Bustad HJ, Flydal MI, Mariaule V, Alvira S, Cuéllar J, Haavik J, Soulé
884 J, Valpuesta JM, Márquez JA, Martinez A, Bramham CR (2015) Arc is a flexible modular
885 protein capable of reversible self-oligomerization. Biochem J. 468:145-158.

886 Newpher TM, Ehlers MD (2008) Glutamate receptor dynamics in dendritic microdomains.
887 Neuron. 58:472-497.

888 Okuno H, Akashi K, Ishii Y, Yagishita-Kyo N, Suzuki K, Nonaka M, Kawashima T, Fujii H,
889 Takemoto-Kimura S, Abe M, Natsume R, Chowdhury S, Sakimura K, Worley PF, Bito H
890 (2012) Inverse synaptic tagging of inactive synapses via dynamic interaction of Arc/Arg3.1
891 with CaMKIIbeta. Cell. 149:886-898.

892 Peden AA, Rudge RE, Lui WW, Robinson MS (2002) Assembly and function of AP-3
893 complexes in cells expressing mutant subunits. J Cell Biol. 156:327-336.

894 Plant K, Pelkey KA, Bortolotto ZA, Morita D, Terashima A, McBain CJ, Collingridge GL,
895 Isaac JT (2006) Transient incorporation of native GluR2-lacking AMPA receptors during
896 hippocampal long-term potentiation. Nat. Neurosci. 9:602-4.

897 Rial Verde EM, Lee-Osbourne J, Worley PF, Malinow R, Cline HT (2006) Increased
898 expression of the immediate-early gene arc/arg3.1 reduces AMPA receptor-mediated
899 synaptic transmission. Neuron. 52:461-474.

900 Robinson MS (2004) Adaptable adaptors for coated vesicles. Trends Cell Biol. 14:167-174.

901 Roy A, Kucukural A, Zhang Y (2010) I-TASSER: a unified platform for automated protein
902 structure and function prediction. Nat. Protoc. 5: 725-738.

903 Saheki Y, De Camilli P (2012) Synaptic vesicle endocytosis. Cold Spring Harb. Perspect.
904 Biol. 4:a005645.

905 Schmid EM, Ford MG, Burtey A, Praefcke GJ, Peak-Chew SY, Mills IG, Benmerah A,
906 McMahon HT (2006) Role of the AP2 beta-appendage hub in recruiting partners for clathrin-
907 coated vesicle assembly. PLoS Biol. 4:e262.

908 Sheffield P, Garrard S, Derewenda Z (1999) Overcoming expression and purification
909 problems of RhoGDI using a family of "parallel" expression vectors. Protein Expr. Purif. 15:
910 34-39.

911 Shepherd JD, Rumbaugh G, Wu J, Chowdhury S, Plath N, Kuhl D, Huganir RL, Worley PF
912 (2006) Arc/Arg3.1 mediates homeostatic synaptic scaling of AMPA receptors. Neuron.
913 52:475-484.

914 Slepnev VI, Ochoa GC, Butler MH, De Camilli P (2000) Tandem arrangement of the clathrin
915 and AP-2 binding domains in amphiphysin 1 and disruption of clathrin coat function by
916 amphiphysin fragments comprising these sites. J. Biol. Chem. 275:17583-17589.

917 Steward O, Wallace CS, Lyford GL, Worley PF (1998) Synaptic activation causes the mRNA
918 for the IEG Arc to localize selectively near activated postsynaptic sites on dendrites. Neuron.
919 21:741-751.

920 ter Haar E, Harrison SC, Kirchhausen T (2000) Peptide-in-groove interactions link target
921 proteins to the beta-propeller of clathrin. Proc. Natl. Acad. Sci. U.S.A. 97:1096–1100.

922 Traub LM, Bonifacino JS (2013) Cargo recognition in clathrin-mediated endocytosis. Cold
923 Spring Harb. Perspect. Biol. 5:a016790.

924 Waung MW, Pfeiffer BE, Nosyreva ED, Ronesi JA, Huber KM (2008) Rapid translation of
925 Arc/Arg3.1 selectively mediates mGluR-dependent LTD through persistent increases in
926 AMPAR endocytosis rate. Neuron. 59:84-97.

927 Zhang W, Wu J, Ward MD, Yang S, Chuang YA, Xiao M, Li R, Leahy DJ, Worley PF (2015)
928 Structural basis of arc binding to synaptic proteins: implications for cognitive disease.
929 Neuron. 86:490-500.

930

931 **Figure Legends**

932 **Figure 1. Arc directly interacts with the AP-2 complex.**

933 (a) Arc co-immunoprecipitates with the α subunit of AP-2. Hippocampal lysate was subjected
934 to immunoprecipitation (IP) with an Arc antibody followed by immunoblot (IB) using an anti-α
935 adaptin antibody. Ten percent of the protein lysate used for the IP was loaded in the input
936 lane. (b) Arc co-immunoprecipitates with clathrin in hippocampal lysate. Hippocampal lysate
937 was subjected to immunoprecipitation (IP) with a rabbit anti-Arc or a normal rabbit anti-IgG
938 control antibodies followed by immunoblot (IB) using an anti-α adaptin and an anti-clathrin

heavy chain antibodies. Ten percent of the protein lysate used for the IP was loaded in the input lane. (c-d) Pull-down assay showing the interaction of AP-2 core with mouse $Arc_{(WT)}$. Recombinant affinity purified GST-AP-2 core (GST tagged α subunit (residues 1-621), 6xHis tagged β2 subunit (residues 1-591), full length μ2 and σ2 subunits), was immobilized on glutathione beads (c, right panel) and incubated with recombinant affinity purified 6xHis-$Arc_{(WT)}$ (c, left panel). Binding of Arc protein to GST-tagged AP-2 core or GST alone was analysed by GST pull-down and SDS-PAGE, followed by Coomassie blue staining (d, left panel) or immunoblot using an anti-Arc antibody (d, right panel). (e) Schematic representation of the Arc-WT sequence showing the truncated Arc mutants used in this study. The diagram indicates coiled-coil (CC) and spectrin repeat homology (SRH) structure domain of mouse Arc. AP-2 binding site is shown in black. (f) Pull-down assay showing the interaction of AP-2 core with mouse $Arc_{(WT)}$ and the $Arc_{(1-199)}$ truncated (deletion of residues 200-396). Recombinant affinity purified AP-2 core, was immobilized on glutathione beads and incubated with lysates of E. coli expressing $Arc_{(WT)}$ or $Arc_{(1-199)}$ deletion mutant. Binding of Arc proteins to GST-tagged AP-2 or GST alone was analysed by GST pull-down and SDS-PAGE, followed by Coomassie blue staining (left panel) or immunoblot using an anti-His tag antibody (right panel). Ten percent of the recombinant proteins used for the pull-down was loaded on the input lane (Bands corresponding to Arc proteins are indicated by white asterisks). (g) Pull-down assay showing that the Arc residues 195-199 are required for the Arc/AP-2 interaction as truncated $Arc_{(1-194)}$ produced in E. coli lost the ability to bind immobilised recombinant GST-tagged AP-2 core.

Figure 2: Identification of Arc motif that binds to AP-2.

(a) Pull-down assay showing that a conserved tryptophan residue at position 197 mediates Arc/AP-2 interaction. Recombinant GST-$Arc_{(WT)}$, GST-$Arc_{(W197A)}$, GST-$Arc_{(195-199A)}$ or GST alone were produced in E. coli and immobilized on glutathione beads (bottom) and incubated with total brain tissue lysate. Binding of endogenous μ2 and α-adaptins to GST fusion proteins was analysed by SDS-PAGE immunoblotting with anti-μ2 (top) or anti-α (middle)

antibodies. Bar chart plotting analysis of the relative amount of protein bound to GST and GST-$Arc_{(W197A)}$ and GST-$Arc_{(195\text{-}199A)}$ normalized to GST-ArcWT (100%). (b) Pull-down assay showing interaction of $Arc_{(WT)}$ and $Arc_{(W197A)}$ with dynamin 2. Recombinant GST-$Arc_{(WT)}$, GST-$Arc_{(W197A)}$ or GST alone were produced in E. coli, immobilized on glutathione beads (bottom) and incubated with total lysates of HEK293 cells expressing dynamin 2-GFP. Binding of dynamin 2-GFP to GST fusion proteins was analysed by SDS-PAGE immunoblotting with anti-GFP antibody (top). Bar chart plotting analysis of the relative amount of dynamin 2 bound on the beads normalized to GST-ArcWT (100%). 10% of total protein lysate used to incubate the beads was used as input. (c) Pull-down assay showing interaction of $Arc_{(WT),}$ $Arc_{(W197A)}$ and GST-$Arc_{(195\text{-}199A)}$ with Triad3A. Recombinant GST proteins produced in E. coli and immobilized on glutathione beads (bottom) were incubated with total lysates of HEK293 cells expressing GFP-Triad3A. Binding of GFP-Triad3A to GST fusion proteins was analyzed by SDS-PAGE immunoblotting with anti-GFP antibody (top). Bar chart plotting analysis of the relative amount of Triad3A bound on the beads normalized to GST-ArcWT (100%). 10% of total protein lysate used to incubate the beads was used as input. Errors bars represent the means ± SEM (n=3 independent experiments). *p<0.05, **p<0.005 and ***p<0.0005 using unpaired Student´s t test.

Figure 3. Arc/AP-2 interaction regulates GluA1 endocytosis

(a,b) Representative blots showing that $Arc_{(WT),}$ but not the $Arc_{(W197A)}$ mutant, facilitates GluA1, but not GluA2 endocytosis. H4 neuroglioma cells were transfected with plasmids encoding myc-GluA1 (a) or myc-GluA2 (b) in combination with either: empty pCIneo vector, pCIneo $Arc_{(WT)}$ or pCIneo $Arc_{(W197A)}$. Western blot band densitometry analysis showing that: (a) $Arc_{(WT),}$ but not $Arc_{(W197A),}$ promotes a significant reduction in surface expression of GluA1 subunits (control: 60.46 ± 2.97%; $Arc_{(WT):}$ 38.55 ± 7.44%; $Arc_{(W197A)}$: 50.18 ± 8.34%. Error bars represent the means ± SEM (n=3 independent experiments). *p<0.05 using one-way ANOVA followed by Tukey´s post-test. (b) $Arc_{(WT)}$ does not promote any changes in surface expression of either GluA2 subunits (control: 132.9 ± 26.66%; $Arc_{(WT)}$): 133.2 ± 21,78%;

Arc$_{(W197A)}$: 143.9 ± 38.43%) or EGF receptor (control: 51.35 ± 10.43%; Arc$_{(WT)}$: 38.93 ± 8,66%; Arc$_{(W197A)}$: 41.59 ± 8.8%). Error bars represent the means ± SEM (n=4 independent experiments).Ten percent of the protein lysate used for incubate the beads was loaded in the input lane. GAPDH was used as loading controls. (c-f) H4 cells co-expressing myc-GluA1 with either mCherry construct alone (c); mCherry-Arc$_{(WT)}$ (d); or mCherry-Arc$_{(W197A)}$ (e). Surface myc-GluA1 (non-permeabilized cells, green channel) was identified using mouse anti-myc antibody followed by Alexa 488 secondary antibody and internal myc-GluA1 (permeabilized, magenta channel) was identified by polyclonal rabbit anti-myc antibody followed by Alexa 647 secondary antibody. (f,g) The mean florescence intensity (MFI) of Alexa488 (surface my-GluA1) and mCherry (red channel) were calculated using confocal Z-projection images to quantify the pixel intensity of surface myc-GluA1 and mCherry (total protein expression). (f) Ratio of averaged MFI between surface (488)/total protein (mCherry) for control cells (n=59 cells) was set to 100 % to facilitate comparison. Note that the ratio for surface GluA1 is significantly reduced in cells expressing mCherry-Arc$_{(WT)}$ 34,68 ± 3,13%; n= 60 cells) compared to cells expressing mCherry construct alone. Importantly, this reduction is absent in cells expressing the mCherry-Arc$_{(W197A)}$ construct (114,80 ± 13,08%; n= 42 cells. (g) Bar chart plotting the averaged MFI expression levels of mCherry-Arc$_{(WT)}$ and mCherry-Arc$_{(W197A)}$ compared to mCherry expression. Values are the mean ± SEM (n=3 independent experiments). *p<0.05; ***p<0.005 using one-way ANOVA followed by Tukey´s posttest. Scale bar=10 µm. (h) Representative blot and bar chart plotting bands densitometry analysis of Arc expression protein in H4 cells transfected with equal amounts of mCherry-Arc$_{(WT)}$, mCherry-Arc$_{(W197A)}$,or mCherry-Arc$_{(195\text{-}199A)}$ plasmids. Note the similar levels Arc protein expression between samples. Values are the mean ± SEM (n=3 independent experiments).

Figure 4. The Arc/AP-2 interaction regulates AMPAR-mediated synaptic currents

(a-d) Representative live imaging of a dissociated hippocampal neuron overexpressing Arc-GFP-tagged constructs and GFP. (a) AMPAR-mediated mEPSC traces from a neuron overexpressing Arc$_{(WT)}$ and an untransfected neighboring neuron. (ai) Amplitude probability

distribution for the mEPSCs shown in (a). Note the shift to the left and increase in the amplitude of the main peak in the neuron overexpressing $Arc_{(WT)}$, clearly demonstrating the reduction in mEPSC amplitude. Inset, superimposed average mEPSC waveforms. (b) Representative AMPAR-mediated mEPSC traces from a neuron overexpressing GFP and an untransfected neighboring neuron. (bi) Amplitude probability distributions for mEPSCs recorded from the neurons shown in (b). Inset, superimposed average mEPSC waveforms. (c) Representative AMPAR-mediated mEPSC traces from a neuron expressing $Arc_{(W197A)}$ and an untransfected neighbouring neuron. (ci) Amplitude probability distributions from neurons shown in (c). Note that expression of $Arc_{(W197A)}$ produced a smaller reduction in mEPSC amplitude compared to $Arc_{(WT)}$ overexpression. Inset, superimposed average mEPSC waveforms. (d) Representative AMPAR-mediated mEPSC traces from a neuron expressing $Arc_{(195\text{-}199A)}$ and an untransfected neighboring neuron. (di) Amplitude probability distributions from neurons shown in (d). Note that expression of $Arc_{(195\text{-}199A),}$ in which the sequence 195QSWGP199 of Arc was mutated to 195AAAAA199 had little effect on mEPSC amplitude. Inset, superimposed average mEPSC waveforms. (e) Cumulative probability distributions for cells expressing $Arc_{(WT)}$ (12 neurons), $Arc_{(W197A)}$ (13 neurons), $Arc_{(195\text{-}199A)}$ (10 neurons), GFP (7 neurons) and for untransfected cells (20 neurons). (f), Bar chart plotting mean mEPSC amplitude for the cells in (e). Expression of $Arc_{(WT)}$ significantly reduced mEPSC amplitude (mean reduced from 15.99 ± 0.9 pA in untransfected cells to 10.56 ± 0.66 pA, p= 0.0002) whereas expression of $Arc_{(W197A)}$ or $Arc_{(195\text{-}199A)}$ had no significant effect (14.6 ± 0.74 pA, p=0.12 and 14.01 ± 1.2 pA, p= 0.37). Expression of eGFP had no significant effect (p=0.376) on the mean mEPSC amplitude compared to untransfected cells. (g) Bar chart plotting the mean interval between mEPSCs. Expression of $Arc_{(WT)}$ and the Arc mutants had no significant effect on the frequency of mEPSCs. Although the mean frequency of mEPSCs in cells expression $Arc_{(WT)}$ appeared reduced, this was not significant as there was large variability between cells. (h) Representative average mEPSC waveforms recorded at a holding potential of -60 and + 40 mV for cells expressing GFP, $Arc_{(WT)}$ and $Arc_{(W197A)}$ in the presence of spermine (100 μM) in the intracellular solution. (i) Bar chart

plotting the mean rectification index (peak amplitude at + 40 mV divided by peak amplitude at -60 mV) for neurons expressing GFP (n = 9 cells; 0.34 ± 0.015), $Arc_{(WT)}$ (n = 9 cells; 0.62 ± 0.016) and $Arc_{(W197A)}$ (n = 6 cells; 0.45 ± 0.015). Thus $Arc_{(WT)}$ reduces the amount of rectification (as seen as an increase in the rectification index) whereas $Arc_{(W197A)}$ has significantly less effect on rectification. Error bars in f, g and i are SEMs ***p<0.001; **p<0.01. Statistical significance was tested using the Mann-Whitney test. Scale bar=10 μm

Figure 5. Overexpression of Arc-cDNAs does not affect AMPAR-mediated mEPSC kinetics in hippocampal neurons

(a) Average of 75 miniature excitatory postsynaptic currents (mEPSCs, aligned on the mid-point of the rising phase) from an individual neuron expressing $Arc_{(WT).}$ The decay was fitted with a single exponential (τ = 4.5 ms, black line). Inset: the average mEPSC at an expanded time-base showing the exponential fit to the decay. (b) Average of 80 mEPSCs (aligned on the mid-point of the rising phase) from an untransfected neuron which was a close neighbour to the cell in (A).The decay of the mEPSC was very similar to the transfected neighbour (the decay was fitted with a single exponential; τ = 4.7 ms, black line). Inset: the average mEPSC at an expanded time-base to show the exponential fit to the decay. (c) Bar chart plotting the mean 10-90 % rise-time of mEPSCs recorded from untransfected neurons (n= 18) and from neurons expressing different constructs and in different conditions (n = 6 for each). The mean rise-time was calculated by averaging the rise-time of mean currents from individual recordings. There was no significant difference in the mean mEPSC rise-time recorded from any of the neurons. (d) Bar chart plotting the mean decay time constant (τ) from untransfected neurons (n=18) and from neurons expressing different constructs and in different conditions (n=6 for each). The mean decay time constant (τ) was calculated by averaging the time constant from the decay of mean currents from individual recordings. The decay of mEPSCs was not significantly different between conditions. The error bars in (c) and (d) are SEMs. Statistical significance was tested using the Mann-Whitney test

Figure 6. AP-2 is required for Arc-dependent changes in synaptic strength

(a) Blots showing levels of μ2 protein obtained from NSC cells overexpressing negative control (n.c.) shRNA, μ2-shRNA$_2$, μ2-shRNA$_3$ plasmids for 3-4 days. GAPDH was used as loading control. Bar chart plotting the analysis of μ2 band intensity normalised by GAPDH. Error bars indicate ± SEM and significance was tested using one-way ANOVA ***p=0.0001. (b) Blots showing levels of μ2 protein obtained from cultured hippocampal neurons infected for 8-9 days with lentiviruses expressing either μ2-nc shRNA or μ2-shRNA$_2$ sequences for 8-9 days. GAPDH was used as loading control. Bar chart plotting the analysis of μ2 band intensity normalised by GAPDH intensity. Error bars indicate ± SEM and significance was tested using One-Way ANOVA, *p=0.019. (c) Representative AMPAR-mediated mEPSC traces from a neuron expressing μ2-shRNA$_2$ and an untransfected neighbour. (ci) Amplitude probability distributions from the neuron shown in (c). Note that reduction of AP-2 expression (μ2-shRNA$_2$) has little effect on mEPSC amplitude. Inset, superimposed average mEPSC waveforms. (d) Representative AMPAR-mediated mEPSC traces from a neuron co-expressing Arc$_{(WT)}$ and nc shRNA and an untransfected neighbour. (di) Amplitude probability distribution from the neurons in (d). Note that co-expression of a n.c. shRNA does not prevent overexpression of Arc from reducing mEPSC amplitude. Inset, superimposed average mEPSC waveforms. (e) Representative AMPAR-mediated mEPSC traces from a neuron co-expressing Arc$_{(WT)}$ and μ2-shRNA$_2$ and an untransfected neighbor. (e(i)) Amplitude probability distribution from the neurons showed in (e). Note that co-expression of μ2-shRNA$_2$ prevents the effects of Arc$_{(WT)}$ on mEPSC amplitude. Inset, superimposed average mEPSC waveforms. (f) Cumulative probability distributions for cells expressing shRNA$_2$ (9 neurons), Arc$_{(WT)}$ + shRNA$_2$ (16 neurons), Arc$_{(WT)}$+n.c shRNA (7 neurons), and for untransfected cells (12 neurons). (g) Bar chart plotting mean mEPSC amplitude for the cells in (f). Expression of shRNA$_2$ prevented the Arc$_{(WT)}$ overexpression effect of significantly reducing mEPSC amplitude (mean mEPSC amplitude 15.3 ± 1 pA in untransfected cells, Arc$_{(WT)}$ + shRNA$_2$ 14.3 ± 0.8 pA, p=0.52). Expression of shRNA$_2$ alone had no significant effect on mEPSC amplitude (13 ± 0.7 pA, p=0.07) whereas Arc$_{(WT)}$ + n.c. shRNA significantly reduced mEPSC amplitude (10.2 ± 0.53 pA, p=0.001). (h) Bar chart plotting the mean

interval between mEPSCs for the cells in (f). The error bars in (g) and (h) are SEMs ***p<0.001; **p<0.005. Statistical significance was tested using the Mann-Whitney test. (i) Amplitude probability distributions for a neuron expressing µ2-shRNA$_3$ and an untransfected neighbour and for a neuron overexpressing Arc$_{(WT)}$ with µ2-shRNA$_3$ and an untransfected neighbour (j). Inset, superimposed average mEPSC waveforms. (k) Bar chart of mean mEPSC amplitudes for untransfected cells (n = 8), cells transfected with µ2-shRNA$_3$ (n=10) and cells transfected with Arc$_{(WT)}$+ µ2-shRNA$_3$ (n=6). Neither expression of µ2-shRNA$_3$ or Arc$_{(WT)}$+µ2-shRNA$_3$ significantly changed mEPSC amplitude (p=0.68 and p=0.27 respectively).

Figure 7. Arc/AP-2µ interaction is required for the Arc-mediated reduction in AMPAR mEPSC amplitude

(a) Representative AMPAR-mediated mEPSC traces from a neuron expressing Arc$_{(WT)}$+µ2-shRNA$_2$+µ2 and an untransfected neighboring neuron. (ai) Amplitude probability distributions from the neurons showed in (a). Note that re-introduction of µ2 rescued the effect of Arc$_{(WT)}$ overexpression leading to a reduction in the amplitude of mEPSC amplitudes (shift to the left, red trace). Inset, superimposed average mEPSC waveforms. (b) Representative AMPAR-mediated mEPSC traces from a neuron expressing Arc$_{(195\text{-}199A)}$+µ2-shRNA$_2$+µ2 and an untransfected neighboring neuron. (bi) Amplitude probability distributions from the neurons showed in (d). Note that re-introduction of µ2 has little effect in mEPSC amplitude (no shifts between black and red traces). Inset, superimposed average mEPSC waveforms. (c) Cumulative probability distributions for cells expressing Arc$_{(WT)}$ +µ2-shRNA$_2$ +µ2 (14 neurons), Arc$_{(195\text{-}199A)}$ +µ2-shRNA$_2$ +µ2 (9 neurons) and untransfected cells (14 neurons). (d) Bar chart plotting mean mEPSC amplitude for the cells in (c). Expression of µ2 rescued the reduction in mEPSC amplitude produced by Arc$_{(WT)}$ overexpression, following the knockdown of AP-2 by shRNA$_2$ (mean mEPSC amplitude in untransfected cells 16.9 ± 1.3 pA vs 10.1 ± 0.6 pA in cells expressing Arc$_{(WT)}$ +µ2-shRNA$_2$ +µ2, p=0.0001). In contrast,

1129 expression of μ2 had no significant effect on mEPSC amplitude when $Arc_{(195-199A),}$ which
1130 does not interact with AP2, was expressed together with $shRNA_2$ (15.9 ± 1.7 pA, p = 0.46).
1131 (e) Bar chart plotting the mean interval between mEPSCs for the cells in (c). The error bars
1132 in (d) and (e) are SEMs ***p<0.001; **p<0.01. Statistical significance was tested using the
1133 Mann-Whitney test.

1134 **Figure 8. AP-2 is required for Arc-dependent homeostatic scaling**

1135 (a) Average mEPSC waveforms from an untransfected neuron cultured in control conditions,
1136 from an untransfected neuron exposed to bicuculline and from a μ2-$shRNA_2$ expressing
1137 neuron that has been incubated in bicuculline (40 μM; 48 hr). Note that the bicuculline-
1138 induced down regulation of the mEPSC amplitude was reduced in AP-2 depleted cells (μ2-
1139 $shRNA_2$ expressing cells).The untransfected neuron and the neuron expressing μ2-$shRNA_2$
1140 that were cultured in the presence of bicuculline were neighbors in the same dish, while the
1141 untransfected neuron cultured in control conditions was from the same preparation. (b)
1142 Cumulative amplitude distribution for untransfected neurons cultured in control conditions
1143 (black line, n=10 neurons), untransfected neurons incubated in bicuculline (red line, n=15
1144 neurons), μ2-$shRNA_2$ expressing cells incubated in bicuculline (blue line, n=6 neurons) and
1145 cells transfected with n.c. shRNA incubated in bicuculline (green line, n=5 neurons). (c) Bar
1146 chart plotting the mean mEPSC amplitude for the cells shown in (b). Incubation in bicuculline
1147 significantly reduced the mean mEPSC amplitude (from 17.3 ± 1 pA to 11.9 ± 0.2 pA,
1148 p=0.0001). Expression of $shRNA_2$ significantly increased mEPSC amplitude in bicuculline
1149 (14.38 ± 0.16 pA, p=0.0001) whereas n.c shRNA had significantly less effect (12.9 ± 0.28
1150 pA, p=0.007). (d) Bar chart plotting the mean interval between mEPSCs for the cells in (b
1151 and c). The error bars in (c) and (d) are SEMs ***p<0.001; **p<0.01. Statistical significance
1152 was tested using the Mann-Whitney test.

1153 **Figure 9. Arc/AP-2 interaction controls synaptic strength**.

The proposed model showing the mechanism by which Arc/AP-2 interaction facilitates AMPAR endocytosis. An increase in neuronal activity promotes rapid Arc mRNA translation and protein expression at the dendritic spines. (1) Newly expressed Arc binds to the AP-2 complex and may activate/facilitate AP-2 interaction with AMPAR at the plasma membrane. (2) To initiate the formation of the clathrin-coated assembly AP-2 binds and recruits clathrin to the membrane. (3-4) Arc then binds and recruits endophilin and dynamin to promote scission of the endocytic vesicle containing the AMPAR to be targeted for either recycling or degradation.

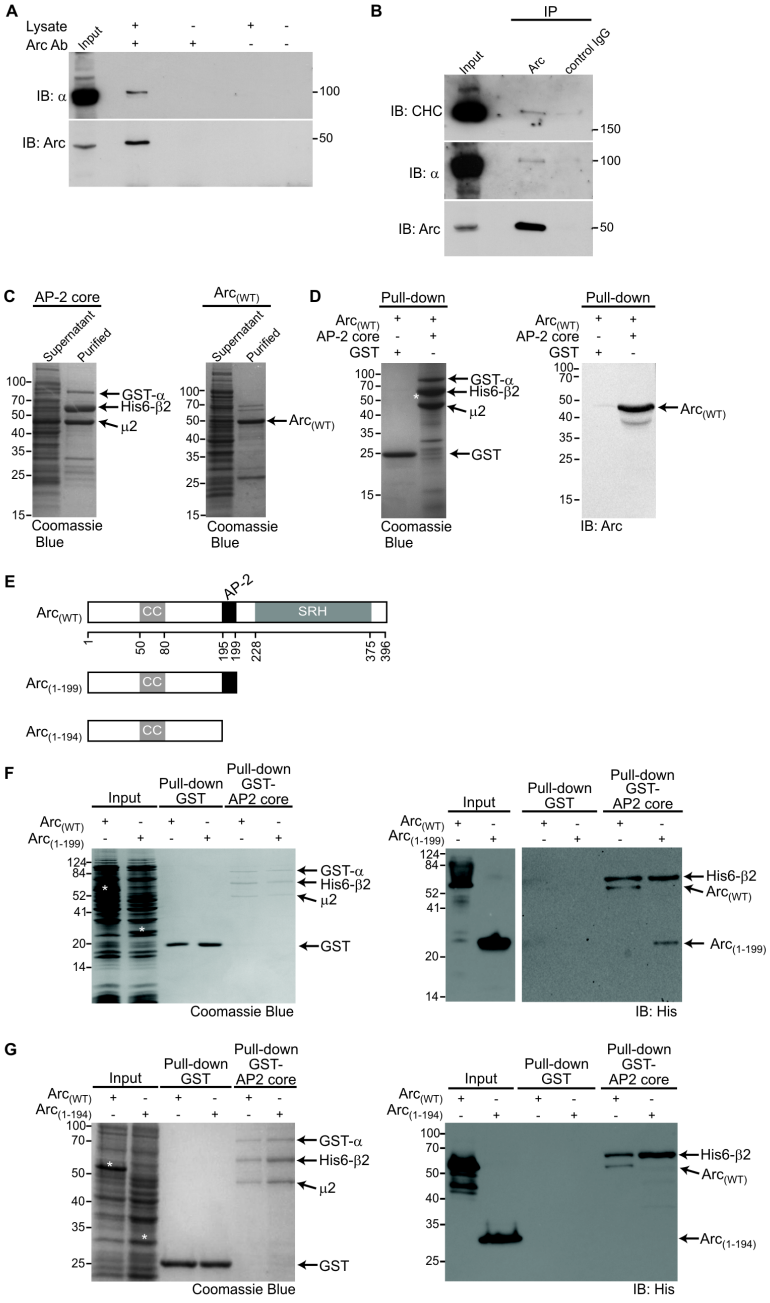

Figure 1

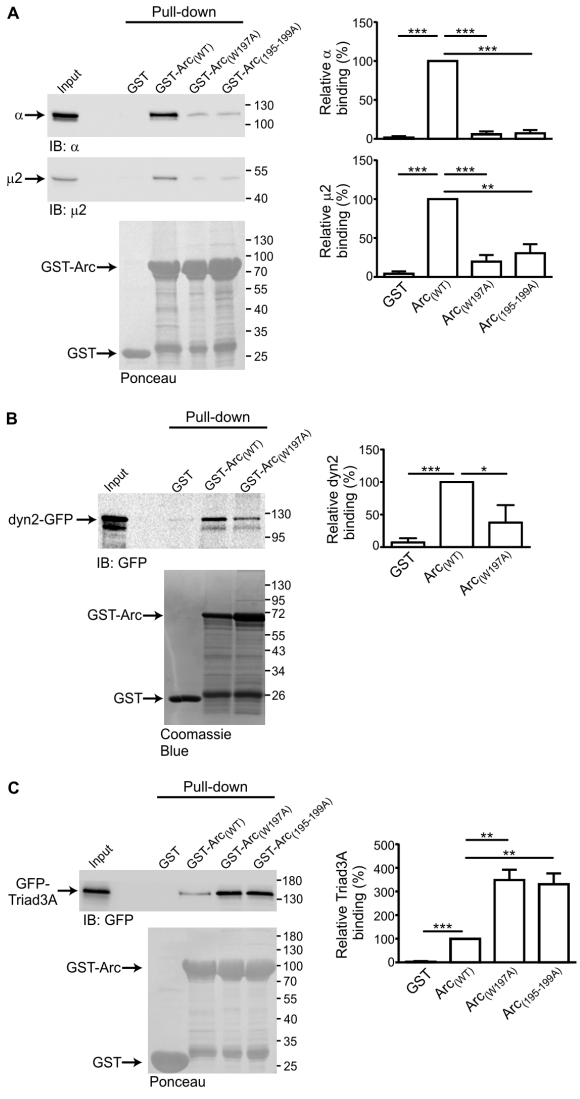

Figure 2

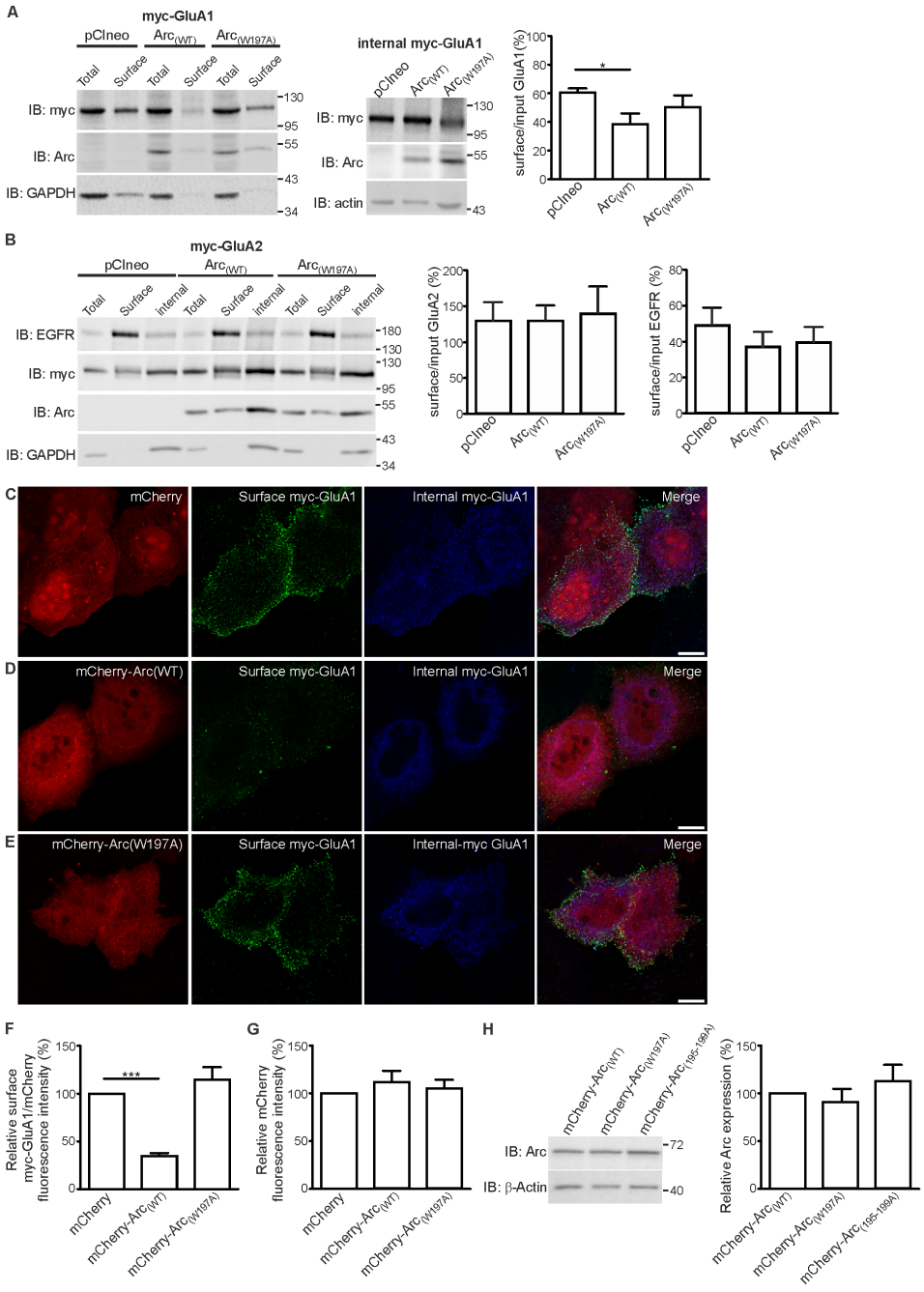

Figure 3

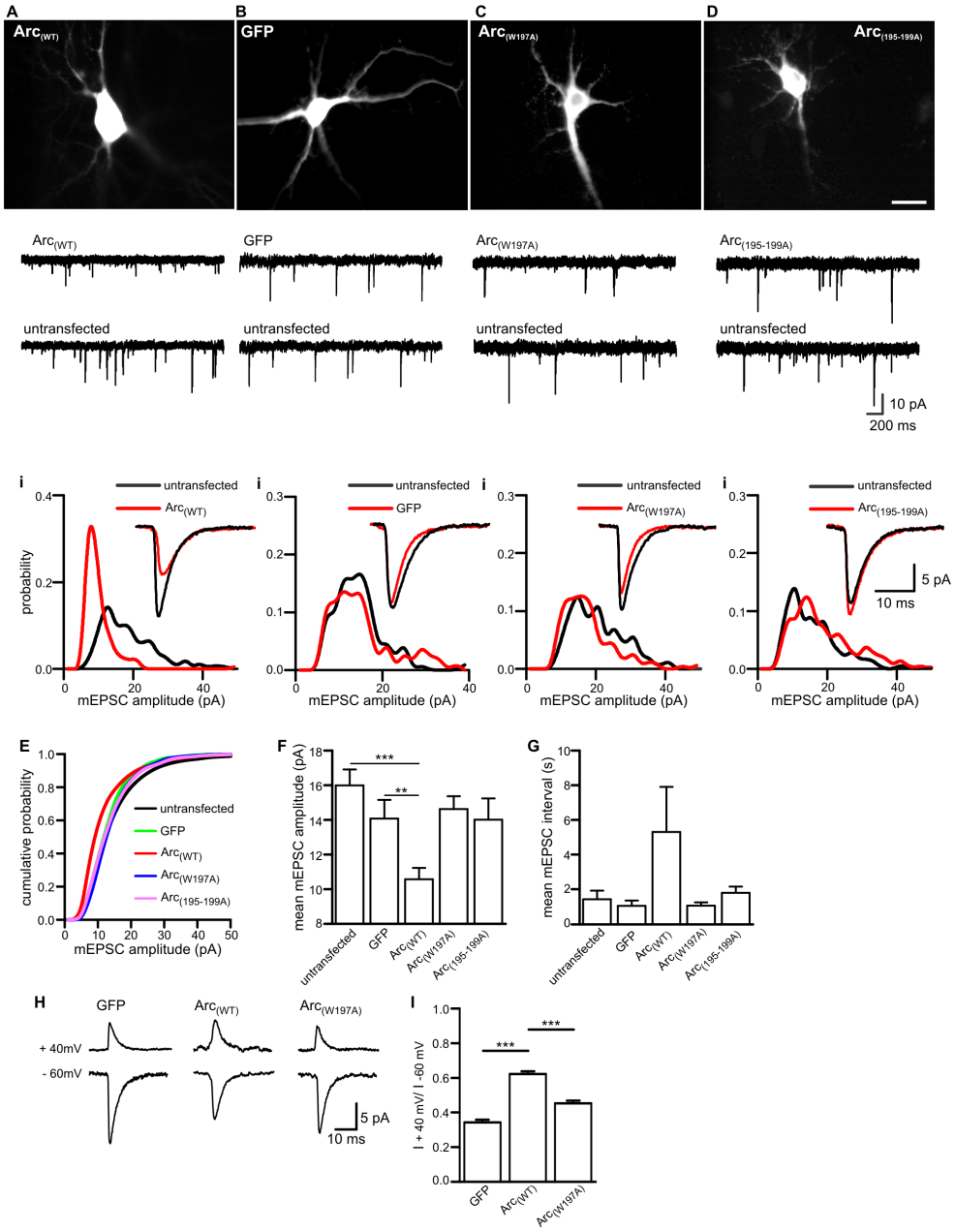

Figure 4

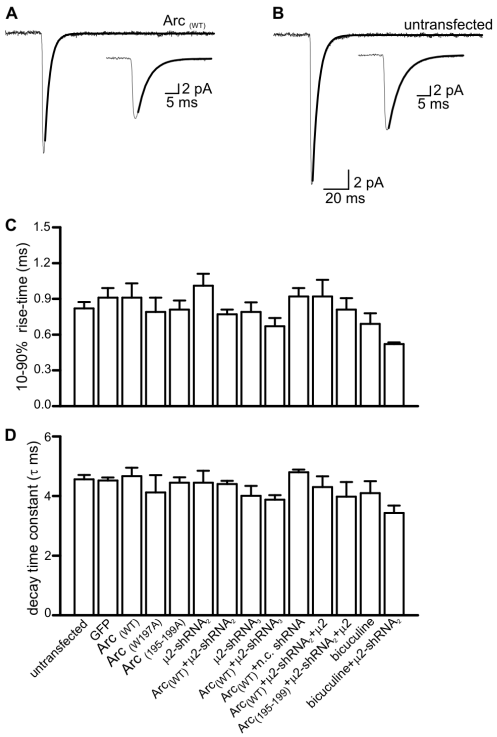

Figure 5

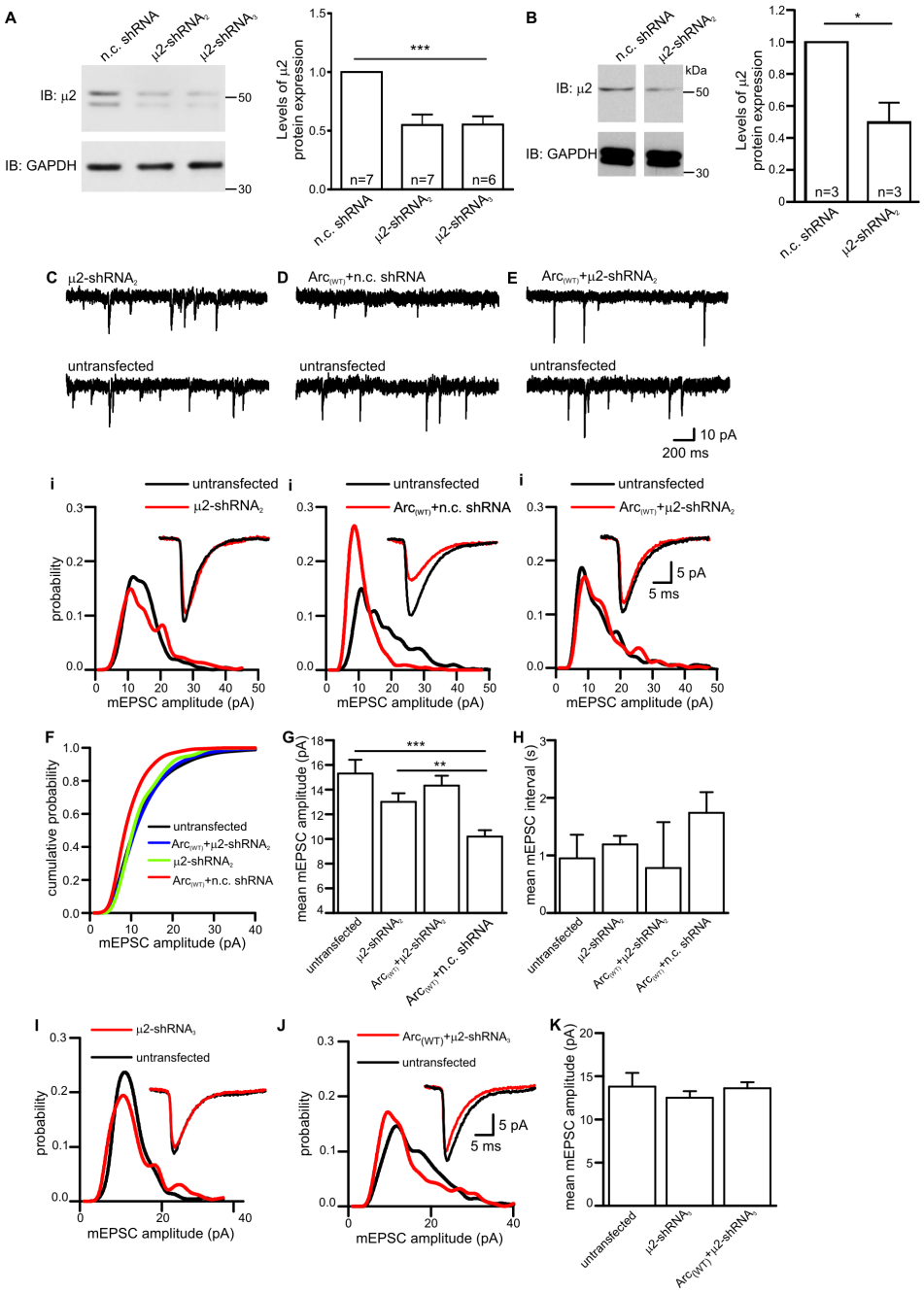

Figure 6

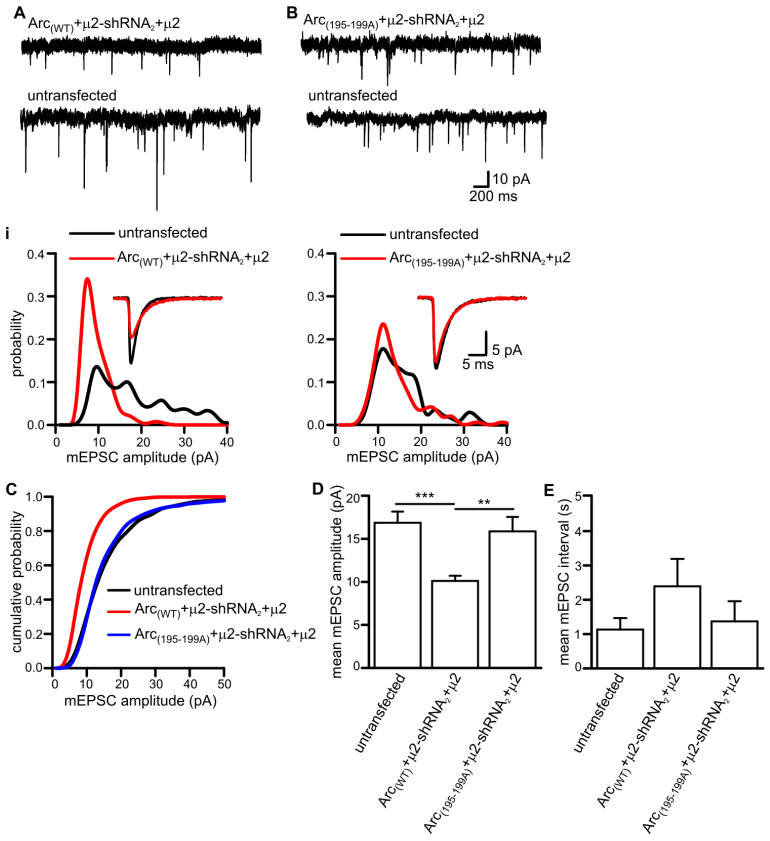

Figure 7

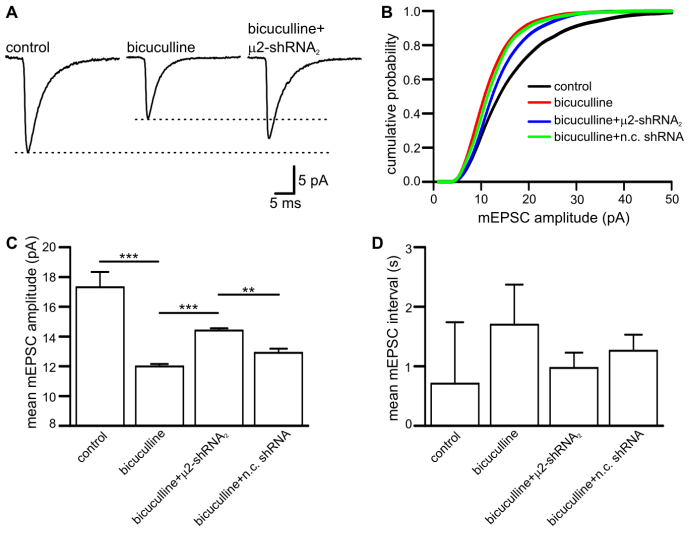

Figure 8

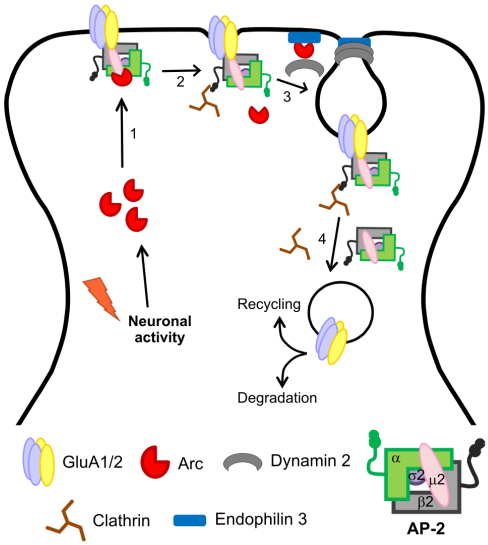

Figure 9

Table1: Statistical Analyses

Results		Data Structure	Type of Test	*n* numbers	Probability (P)
(Fig. 2a, top panel) IB pulldown α	GST-Arc$_{(WT)}$ vs GST	Two factor, mean	t test	3/3	< 0.0001
	GST-Arc$_{(WT)}$ vs GST-Arc$_{(W197A)}$	Two factor, mean	t test	3/3	< 0.0001
	GST-Arc$_{(WT)}$ vs GST-Arc$_{(195\text{-}199A)}$	Two factor, mean	t test	3/3	< 0.0001
(Fig. 2a, middle panel) IB pulldown μ2	GST vs GST-Arc$_{(WT)}$	Two factor, mean	t test	3/3	< 0.0001
	GST-Arc$_{(WT)}$ vs GST-Arc$_{(W197A)}$	Two factor, mean	t test	3/3	0.0007
	GST-Arc$_{(WT)}$ vs GST-Arc$_{(195\text{-}199A)}$	Two factor, mean	t test	3/3	0.0039
(Fig. 2b) IB pulldown dyn2-GFP	GST-Arc$_{(WT)}$ vs GST	Two factor, mean	t test	3/3	< 0.0001
	GST-Arc$_{(WT)}$ vs GST-Arc$_{(W197A)}$	Two factor, mean	t test	3/3	0.0159
(Fig. 2c) IB pulldown GFP-Triad3A	GST-Arc$_{(WT)}$ vs GST	Two factor, mean	t test	3/3	< 0.0001
	GST-Arc$_{(WT)}$ vs GST-Arc$_{(W197A)}$	Two factor, mean	t test	3/3	0.0055
	GST-Arc$_{(WT)}$ vs GST-Arc$_{(195\text{-}199A)}$	Two factor, mean	t test	3/3	0.0055
(Fig. 3a) IB Surface GluA1	pCIneo vs pArc$_{(WT)}$	Two factor, mean	ANOVA Tukey's	3/3	0.1284
	pCIneo vs pArc$_{(W197A)}$	Two factor, mean	ANOVA Tukey's	4/4	0.5543
(Fig. 3b) IB Surface GluA2	pCIneo vs pArc$_{(WT)}$	Two factor, mean	ANOVA Tukey's	4/4	>0.9999
	pCIneo vs pArc$_{(W197A)}$	Two factor, mean	ANOVA Tukey's	4/4	0.9637
(Fig. 3b) IB Surface EGFR	pCIneo vs pArc$_{(WT)}$	Two factor, mean	ANOVA Tukey's	4/4	0.6156
	pCIneo vs pArc$_{(W197A)}$	Two factor, mean	ANOVA Tukey's	4/4	0.7621

(Fig. 3f) IF Surface GluA1	mCherry vs mCherry-$Arc_{(WT)}$	Two factor, mean	ANOVA Tukey's	59/60	<0.0001
	mCherry vs mCherry-$Arc_{(W197A)}$	Two factor, mean	ANOVA Tukey's	59/42	0.3438
(Fig. 3g) IF mCherry expression	mCherry vs mCherry-$Arc_{(WT)}$	Two factor, mean	ANOVA Tukey's	3/3	0.5625
	mCherry vs mCherry-$Arc_{(W197A)}$	Two factor, mean	ANOVA Tukey's	3/3	0.9211
(Fig. 3h) IB Arc expression	mCherry-$Arc_{(WT)}$ vs mCherry- $Arc_{(W197A)}$	Two factor, mean	ANOVA Tukey's	3/3	0.6892
	mCherry-$Arc_{(WT)}$ vs mCherry- $Arc_{(195\text{-}199A)}$	Two factor, mean	ANOVA Tukey's	3/3	0.4951
(Fig. 4) Arc/AP-2 interaction	$Arc_{(WT)}$ vs untransfected amplitude frequency	Two factor, mean	Mann Whitney	12/20	 0.0002 0.47
	$Arc_{(W197A)}$ vs untransfected amplitude frequency	Two factor, mean	Mann Whitney	13/20	 0.121 0.98
	$Arc_{(195\text{-}199A)}$ vs untransfected amplitude frequency	Two factor, mean	Mann Whitney	10/20	 0.372 0.18
	eGFP vs untransfected amplitude frequency	Two factor, mean	Mann Whitney	7/20	 0.376 0.39
(Fig. 5) cDNA constructs and mEPSC kinetics	All constructs vs untransfected rise decay	Two factor, mean	Mann Whitney	6/18	 >0.05 >0.05
(Fig. 6) AP-2 requirement for Arc mediated changes in synaptic strength	µ2-$miRNA_2$ vs untransfected amplitude frequency	Two factor, mean	Mann Whitney	9/12	 0.07 0.37
	$Arc_{(WT)}$ + µ2-$miRNA_2$ vs untransfected amplitude frequency	Two factor, mean	Mann Whitney	16/12	 0.52 0.63
	$Arc_{(WT)}$ + n.c.miRNA vs untransfected amplitude frequency	Two factor, mean	Mann Whitney	7/12	 0.001 0.08
	µ2-$miRNA_3$ vs untransfected amplitude frequency	Two factor, mean	Mann Whitney	10/8	 0.68 0.45
	$Arc_{(WT)}$ + µ2-$miRNA_3$ vs untransfected amplitude frequency	Two factor, mean	Mann Whitney	6/8	 0.27 0.14
(Fig. 7) The Arc-AP-2µ interaction is required for Arc-mediated changes in synaptic strength	$Arc_{(WT)}$ +µ2-$miRNA_2$+µ2 vs untransfected amplitude frequency	Two factor, mean	Mann Whitney	14/14	 0.0001 0.37
	$Arc_{(195\text{-}199A)}$+µ2-$miRNA_2$+µ2 vs untransfected amplitude	Two factor, mean	Mann Whitney	9/14	 0.46

	frequency				0.64
(Fig. 8) AP-2 is required for homeostatic scaling.	Control vs bicuculline (untransfected) amplitude frequency	Two factor, mean	Mann Whitney	10/15	 0.0001 0.64
	$miRNA_2$ (bicuculline) vs untransfected (bicuculline) amplitude frequency	Two factor, mean	Mann Whitney	6/15	 0.0001 0.59
	n.c.miRNA (bicuculline) vs untransfected amplitude frequency	Two factor, mean	Mann Whitney	5/15	 0.007 0.29